General Comments from the Authors:

We would like to sincerely thank both reviewers for their instructive comments and we believe the manuscript has been significantly strengthened based on these comments and ideas. We have tried in every instance to incorporate these comments into a revised analysis and manuscript. Responses to each suggestion or questions are given below.

There were two significant errors in the previously submitted manuscript. One of which (pointed out by Dr. De Visscher) is the use of temperature in the Obukhov length and boundary-layer height calculations, where the actual equations specify potential temperature. The second error was the comparisons of Fig. 5 and Table 3 were actually comparisons of effective plume height and not plume rise as stated (i.e. the numbers included stack heights and were hence offset between 76 and 183 m. These errors have been corrected our revised manuscript. Although the numbers have changed due to these corrections, the general findings of the study (that the Briggs equations significantly underestimate the plume rise at this location) is still supported by these new results.

Further, we have expanded on one of Dr. De Visscher's suggestions to disaggregate the results and we used this new analysis to address a number of other reviewer comments and concerns. The revised manuscript now contains a new section in which the comparison of calculated to observed plume rise is redone 24 times, under a variety of separation of data (i.e. comparisons for each stack and for each stability class) as well as variations on the original equations (i.e. alternate plume rise formulae, removal of the minimum functions, different ways to calculate stability, and more). The statistical summary of these comparisons will be presented as a new table in the revised manuscript (following the style of Table 3) and the comparison plots (as Fig 5.) for all 24 cases will be provided as supplementary material. In the comments below, this reanalysis is referred to repeatedly as the "conditions comparison".

Responses to individual reviewer comments follow in blue text.

RC1:

1. In section 2.1 - Authors should provide more explanation on the limits of L used to define stability classes. For example, why the specific lower limits (-0.25hs) applied to L to define unstable conditions?

These limits of z/L are given by Briggs and a citation is added to the text. It is noted that Briggs suggests using the effective stack height ($h_e = h_s + \Delta h$), which would be difficult to code (since stability class becomes dependent on plume rise, which is dependent on stability class). GEM-MACH uses $z = h_s$ instead. In the new "conditions comparison" (see above) we explore the effect of changing the limits of neutral conditions (to both $-8 < \frac{h_s}{L} < 1$ and $-2 < \frac{h_s}{L} < 0.25$). Both these changes result in minimal change in the resulting predicted plume rise, suggesting the analysis is not sensitive to the choice of these parameters.

2. In section 2.3 – Authors should provide more comment/investigation of uncertainties introduced by assuming NPRI inventory values for effluent velocity and exit temperature for the flaring stack.

We have added a comparison using the other CNRL stack (CNRL1), which is a sulphur recovery unit. For CNRL1, both CEMS and NPRI data are available for this period, allowing a direct comparison between the two reporting methods. This comparison demonstrates that the reported NPRI temperature is within 5% of the CEMS temperature, the NPRI reported exit velocity is more than a factor of 4 higher than the CEMS exit velocity. While the flaring stack (CNRL4 in the previous manuscript) may be very different than the sulphur recovery unit stack, this at least provides a rough estimate of the uncertainty due the use of NPRI values.

3. In section 2.3 – Authors should make it clear that stack characteristic values shown in Table 1 are for information purposes only and not used in the actual calculations (presumably hourly stack data was used [emission rates, exit temperatures, exit flow velocities]).

New text has been added to revised manuscript to clarify – both within the main text (2nd paragraph) and the table caption.

4. In section 2.7 – the flights (e.g., box flights) seem to take up to 2 hours and so some measurements during the flight will be time-displaced from other measurements during the flight. Although this is expected, the authors should at least comment that results, such as shown in figure 3(a) actually represent different time periods and that significant evolution of the plume could have occurred during the flight. Are there correction methods for this? How does this affect the measurements?

A paragraph is added (6th paragraph) to discuss the effects of stationarity. Reference is made to Gordon et al. (2015), where the effects are discussed in more detail. It is expected that this would have little effect on the estimated location of the plume centre, especially as the direction of spiraling was not consistent between flights (i.e. the aircraft would sometimes fly in an ascending spiral and sometimes in a descending spiral).

5. In section 2.7, paragraph starting at line #441 – Authors explain attempts to match calculated plumes to observed; was this matching substantiated by say, video-recording of the plume event? Also final sentence of that paragraph states assumption of multiple plumes having merged; was this actually observed in the field as happening? If so, I'd suggest it be noted.

There was no video recording of plume events. Matching is done purely through proximity of observed and parameterized coordinates. Text is added to note that visual observations by the authors during the field work supports the plume merging, especially far downwind of the stacks.

6. In section 4.1, paragraph starting at line 570 – Authors observe a significant difference between Obukhov length-based stability and temperature lapse rate-based stability. It would be useful to have comment on which is the better method to use.

The criteria for stability are now tested in the "conditions comparison" with both Obukhov length and lapse rate (see Table 4). Based on the second reviewer's comments we have also added a comparison of the Pasquil-Gifford stability class. All three methods produce very difference distributions of stability class, but all methods result in a significant underprediction of plume rise by the Briggs equations. Hence the main conclusions of the study are not strongly dependent on the stability calculation used.

7. In section 4.2, 1st paragraph – Authors indicate that they change input variables by an "arbitrary fraction" but it would be better to change them to the reasonable limits of their range; this would then provide a more useful ranking of model sensitivity. Some of the variations they have used do, in fact, seem like reasonable limits so are they truly arbitrary?

This section has been redone so that the variations are calculated based on the difference between the AMS03 and AMS05 towers. The plume rise is then recalculated for the duration of the study modified by this average difference. This demonstrates the sensitivity of the plume rise calculation to the heterogeneity of the variables within the study area. As would be expected there are large differences in the values of H and L calculated with the AMS03 data relative to the values of H and L calculated with the AMS05 data (71% and 165%). There are significant differences in the average plume rise (between –27% and 7%) when the H and L values data are modified by these amounts. We believe this makes the modification less arbitrary, as the data are being modified by an actual difference in measured values, as opposed to a "hand-picked" percentage. We also note that the issue of spatial heterogeneity of the meteorological observations was shown to be of key importance in our companion paper (Akingunola et al), which examines the plume rise equations within the context of a high resolution coupled air-quality/meteorology model (GEM-MACH).

8. In section 5, second paragraph – Authors quote the Webster and Thomas (2002) study implies an underestimation of plume rise based (seemingly) only on an overestimation of surface concentrations. I have not reviewed that study but there can be multiple reasons that a model overestimates ground-level concentrations (for example, overly conservative emission rates). It would be useful for the authors to provide comment on how they discerned that it was only the (presumed) plume rise underestimation that led to those results.

The language used to describe the Webster and Thomas results and their interpretation is modified to emphasize that this is only one possible reason for the overestimation. For example, lines in Section 1 now state “However, there may be other factors…” and in Section 5 “however, there may be other reasons…”.

9. Various references.

Fixed.

RC2 Specific Comments:

Note: Many comments here are essentially criticisms of the Briggs parameterization. These are not meant as criticisms directed at the authors.

We thank the reviewer for this explanation. Generally, we have tried to incorporate as many of these comments as possible into the discussion, especially in light of the poor performance of the Briggs algorithms in this analysis. Whenever possible, the new "conditions comparison" (as discussed above) is used to test some aspects of the parameterization that are pointed out as potentially flawed or inaccurate.

- p. 4 lines 133-134: The authors used the temperature gradient between the surface and the stack tip as a proxy for the temperature gradient above the stack tip. This will cause the atmospheric stability to appear less neutral than it actually is (i.e., more stable, as s is meant to be used in stable atmosphere).

This is how the temperature gradient is calculated in the GEM-MACH model, so we are following this approach here. Text is added here to acknowledge this fact and to point out that the "layered method" described later in Section 2.2 is essentially a test of using known temperature gradients above the stack height.

- p. 4 line 135: when the "maximum" temperature gradient is set at -5 K/km, do you mean -5 is the least negative gradient (i.e., the most stable gradient)? Please provide a reason for this choice, as more stable atmospheres are quite common. Also, it would be useful to test the effect of this restriction on the plume rise predictions.

The –0.005 K/m gradient is in the code statement dTdz=max(dTdz,–0.005), so this value is a minimum - not a maximum as stated (we thank the reviewer for bringing this error to our attention). It is the least stable gradient that can be used to calculate s. This is an approximation of the moist (pseudo) adiabatic lapse rate. The statement is a requirement of both the plume rise algorithms themselves and any attempt to convert them into code, in that the use of this minimum avoids the possibility of a value of $s = 0$ as the environmental lapse rate approaches this limit. Otherwise, the algorithm would give an infinite plume rise if the Obukhov length indicated stable conditions. We have added text to help make this clear, including the resulting condition of $s \geq 0.047/T_a$. The "conditions comparison" tests the analysis without this minimum condition and it is found that the change in predicted to observed plume rise is small.

- eq. 4 p. 4: I realize that most air dispersion models define a final plume rise for unstable atmosphere, but I find this a fundamentally flawed notion: in an unstable atmosphere the plume will continue rising until it either approaches the top of the mixing layer, or gets trapped in a downdraft stronger than the plume's rise. Given this, it is not surprising that the Briggs parameterization tends to underestimate plume rise. I would argue that the parameterization was designed to underestimate plume rise. Given this, it is surprising that earlier studies indicated that the Briggs parameterization overestimated plume rise. It would be useful to gain insight as to why earlier studies found plume rises less than predicted by Briggs. Were these also final plume rise calculations, or transitional plume rise?

This is a very interesting point. However, as noted in a previous comment, the stability class is based on measurements near the surface, without knowledge of conditions further aloft. The details of the previous studies are not clear, but it is noted that most of the corrections are given for neutral conditions only. Based on the shortcomings that the reviewer points out, it would be expected that the "layered method" should perform much better, since this method uses measurements of gradients throughout the mixing layer. If the layered method were used in a fully unstable boundary layer the plume would rise to the top of the mixing layer. This is a better representation of what the reviewer states. But the results show that the layered method actually gives lower plume rise than the Briggs approach, implying that no completely unstable boundary layers were observed in this study.

- eq. 4 seems to predict unrealistically small plume rise when the wind speed is high. Also, depending on what friction velocities are used in unstable vs neutral plume rise, the neutral plume rise equation (eq. 5) often predicts larger plume rise than the unstable plume rise equation. That seems unrealistic to me.

We agree that the Briggs approach seems flawed, but we are testing the parameterization as it appears in the models.

- Eq. 5 p. 5 contains an error. u* in denominator of the last term should be squared. Please check that the calculations were carried out correctly.

This is a typo in the manuscript only and has been corrected. The equation is correct in the programs used for the analysis.

- Eqs. 4 p. 4 and 5 p. 5: the second function of eq. 4 and the first function of eq. 5 are dimensionally not homogeneous, which means they are not supported by similarity considerations, and they will not have a broad validity. Please bear this in mind.

This is true and is another shortcoming of the Briggs equations (or at least the variants used in GEM-MACH).

- For both eq. 4 and eq. 5, the second function of the minimum seems more realistic to me. It would be useful to check if these second functions provide better predictions than the first functions.

This check had already been done as part of the testing described in Section 4.4.1 of the submitted manuscript. It is easy to see how that detail might have been missed, especially as this section appears much later in the paper. This analysis is now included as part of the "conditions comparison". With the revised analysis, it turns out that removing the minimum functions for these data results in unrealistically high plume rises, so use of the minimum functions is recommended as part of the manuscript conclusions.

- An equation that is sometimes used for final plume rise in a neutral atmosphere is 400 Fb/U^3. It might be useful to check if that equation gives any better predictions than eq. 5.

This alternate formula is included as part of the "conditions comparison" analysis. In cases of low wind speeds, it results in extreme values of plume rise. Hence, based on these results its use is not recommended for use.

- eq. 7 only makes sense in a stable atmosphere, because s only has physical meaning in a stable atmosphere. Was it used for stable atmosphere only, or for all types of atmosphere?

Text is added to clarify that the equation is used for only stable and neutral layers ($s = 0$ in a neutral layer). This approach was explained in our companion paper in this special issue (Ayodeji et al.) and that explanation is reproduced in this section. In summary: the plume is assumed to ascend without loss of buoyancy in unstable layers (as with the neutral case). However, it is noted (as discussed in Section 4.1) that the majority of the layers are either neutral or stable (see Table 5).

- p. 6 lines 208-209: For some emissions, it was assumed that the emission profile in 2013 was the same as in 2010. That puts the calculation on shaky ground. Do you really need these data?

The 2010 inventory info was only used to determine SO_2 mass emission rate, not stack parameters, as a means of selecting the stacks with the greatest potential impact on SO_2 concentrations for further analysis. This value is either significant for a stack that emits SO_2, or negligible for a stack that does not. This is the criteria used to reduce the total number of stacks to 8 stacks of interest due to their level of emissions. These values are not used in any calculations – only selection. It was assumed that a stack designed to emit SO_2 in 2010 will still be a significant emitter of SO_2 in 2013. Since the table is reduced to only include the 8 stacks used in the analysis (following the reviewer's suggestion below), the text to explain this has been modified and is hopefully easier to understand.

- Table 1 p. 7: Please indicate which data were collected with CEMS, and which weren't. The CEMS data will be a lot more reliable, and should be treated as such.

Only the CNRL flare stack (originally called CNRL4, now called CNRL2) flow rate and temperature are from NPRI inventory values (i.e. not CEMS). This is labelled in the new table in a way that is easier to see. This stack is also disaggregated from the results in the "conditions comparison" section (as are all the stacks).

- Table 1 p. 7: If I understood correctly, you mention 19 emissions here, but you only used 8 of them. Unless I misunderstood or unless you have a compelling reason to keep all the data in the table, please remove the data that were not used in the test.

The original intention was to demonstrate why we only select the 8 stacks of interest (based on SO_2 emissions and observations). However; we agree with the reviewer that including the statistics for all these unused stacks adds no value to the manuscript, so the explanation for the selection of the 8 stacks is in the text only. The section has been rewritten to more clearly explain the rationale and process of selecting the 8 stacks for analysis.

- eq. 8 p. 7: Why not use an equation based on the momentum flux parameter Fm for plume rise due to momentum? (see p. 22)

We have moved the analysis of momentum from this section. It is discussed in the “conditions comparison” section along with some other parameterizations (including those based on the momentum flux parameter).

- Table 2: Some correlations seem quite low. To what extent is the lack of agreement between the predictions and the measured plume heights due to wind and temperature uncertainties?

We discuss the fact that this is a very inhomogeneous terrain and hypothesize that this is the reason for the low correlation. This will undoubtedly lead to lower agreement between the predicted and measured plume heights, and this may be responsible for the very low correlations between modelled and measured plume rise values (see Table 3). The sensitivity tests (Section 4.2) have been rewritten (see Reviewer 1, comment 7), so that they test what effect the difference between measurement locations can have on the plume rise. While the lack of agreement between predicted and measured plume height may be due to different measurement locations, Fig. 5 and Table 3 demonstrate that all of the measurement locations result in (nearly) the same underprediction of plume rise. In our companion paper (Akingunola et al), we have used a high resolution simulation of the on-line GEM-MACH air-quality model to examine potential impacts of the large level of horizontal variability of the temperature profiles on predicted plume rise, the model having the advantage of providing continuous profiles at the actual stack locations themselves.

- eq. 9 p. 10: Please check if this is correct. Richardson numbers are normally based on the potential temperature, not the actual temperature. Please also check the other variables in the equation and make sure they were interpreted correctly.

This was an error (as discussed in the opening paragraphs of this response). We have corrected the analysis to use potential temperature for both the Richardson number and the boundary-layer height calculations. As discussed above, the main conclusions of the manuscript do not change because of this correction. We have also double checked all the other variables and confirmed that they are correct.

- eq. 10 p. 10: what value of z is used here?

We add the text: “The Obukhov length is calculated from the stability parameter as $L = z_{max}/(z/L)$, where z_{max} is the highest measurement height of 167 m, 90 m, or up to 800 m for AMS03, AMS05, and the RASS respectively.”.

- eq. 10 p. 10: Estimating L without a sensible heat flux measurement or estimation is very difficult. Expect substantial inaccuracies with this equation. This may explain why the values of z0 vary so strongly by location. A value of 10.1 m, for instance, is suspiciously high even for a forest.

We agree this is not a very accurate method for the estimation of L. We have added a paragraph to the text to discuss this. The magnitude of L is not used directly in the Briggs equations, except in the determination of stability class and convective velocity (H_*). The new sensitivity analysis demonstrates that L varies by an average of 165% between the AMS03 and AMS05 stations. We have added text to note that this is likely due to the uncertainties in this equation and also to suggest the potential explanation for the very high z_o value.

- eq. 11 p. 10: Also expect substantial inaccuracies for this equation. At the verge of a temperature inversion, this equation predicts infinite boundary-layer height. In an unstable atmosphere, the boundary layer height is mainly influenced by the accumulated sensible heat deposited into the atmosphere during the current day, so parameterizations such as eq. 11 are questionable in unstable atmospheres.

We also agree this is not a very accurate method for the estimation of H and we have added text to discuss this in the revised manuscript.

- Figure 4 shows a distribution of the calculated plume rise values, for the different calculation schemes and input data. How do these distributions compare with measured plume rise values?

We had been hesitant to do this, as this section was meant as a comparison of plume rise as calculated with data from the various measurement locations. These distributions are for the entire flight period (the 46 hours when box or screen patterns were being flown). The next section then compared the plumes which could be matched to specific stacks. To calculate plume rise from the observations it is necessary to match this plume with an emitting stack so that the stack height can be subtracted from the observed height. Hence what the reviewer asks for here is essentially a comparison of two different things (plume heights for every stack over a 46 hour period versus only matched, observed plume heights).

- p. 16: Comparing the average ratio between predictions and measurements of the plume rise will tend to be biased, because a small number of data points with very low measured plume rise (small denominator) can skew the results upwards. To complement this information, it would be best to also calculate the average calculated plume rise, and compare it with the average measured plume rise. This will tend to give the instances of high plume rise the largest weight, so it is also an imperfect measure. Reporting both average ratio and ratio of the averages will give the reader a good sense of how the measurements compare with the calculations.

Average calculated and average predicted have been added to all the relevant tables and are discussed in the text.

- Figure 5: It could be coincidence, but I have the impression that there is some clustering of the data points, particularly near the x axis (very low predictions irrespective of the actual plume rise). This gives me the impression that some equations within the Briggs parameterization are far less accurate than others. It would be useful to see the performance of each equation separately (even distinguishing between the two equations where a minimum is calculated). Also, if some of these data are based on CEMS and some are based on emission inventory data, it would be useful to know which is which, because the CEMS data will be much more reliable. I realize that I’m asking for a lot of disaggregation here. Perhaps a supplementary document could be prepared alongside the paper.

We agree that this is a lot of disaggregation; however we have attempted to incorporate as much of this reanalysis as possible in the revised manuscript. The CEMS versus NRPI analysis is only the removal of one stack (was CNRL4, is now CNRL2). However, based on this and other comments we have opted to add the new "conditions comparison" analysis (as discussed above) in which the comparison between predicted and observed plume rise has been repeated under multiple new scenarios. As per the reviewer's suggestion, we also present the variation of Figure 5 for each of these variations as supplementary data.

With respect to the clustering noted by the reviewer, this is a results of the error discussed above in which effective plume height was plotted in this figure instead of plume rise. Having fixed this error in the revised manuscript, it is apparent that this is a clustering of very low plume rises (near 0), due to two stacks with very low exit velocity (Suncor 1 and 3 in Table 1). The results are also analyzed without these stacks as part of the "conditions comparison" and the implications are discussed in the revised manuscript.

- Table 4 p. 19: there is a huge discrepancy between the stabilities evaluated from the data of the different sources. This confirms the poor reliability of the calculation scheme for L. If the Pasquill stability classes are known for these measurements, then it might be possible to determine which data set is most reliable.

We have added estimations of the Pasquill stability class to Table 4. As a test of the effect of uncertainty in determining stability class, we have added a reanalysis of the data using lapse rate and Pasquill stability classes to determine the effect of stability classification technique on plume rise. Use of the Pasquill stability class does improved the results somewhat, but there is still an underprediction of plume rise by the Briggs equations with all three techniques (i.e. Obukhov length, lapse rate, and Pasquill class).

- Table 5 p. 20: This sensitivity analysis is very useful, but I find the result suspect. The surface temperature is found to have almost no influence on the plume rise, but the value of H has a large effect. The surface temperature affects H quite strongly, so I don't see how this is possible. Please check.

This analysis was done by changing the value of the available input parameters in the plume algorithm (equivalent to multiplying the predetermined value of $T_{surface}$ or H in the input file). The values are not modified "from the beginning", so H is not recalculated with the modified $T_{surface}$, for example. As the reviewer has noted, this is not exactly correct, so we have recalculated the sensitivity by modifying the variables before all calculations. However, we have changed the analysis to modify $\Delta T = T_a - T_{surface}$ by a given factor (not the surface temperature alone), This demonstrates the relative importance of finding a representative temperature gradient to drive the equations.

- p. 22, top: The authors claim that final plume rise is reached within 2 km in all cases. I find that hard to believe when some plumes rise by 600-800 m. If the Briggs parameterization greatly underestimates plume rise, it will also underestimate the distance to final plume rise. Hence, I would suggest that the authors use the maximum measured plume rise as a guide for estimating the maximum distance to plume rise.

We have added a discussion based on this idea, which we are in agreement with. We have added a calculation of distance to plume rise using the observed values of plume rise from the matching plume. The text is rewritten to incorporate this change and a reanalysis of the data is tested in the “conditions comparison” in which the plumes which are not predicted to reach maximum height at the measurement location are scaled to their predicted height at the measurement location. However, this correction does not appear to affect the overall results significantly.

- p. 22 line 668: Please capitalize letter D in my name and sort my book under D in the reference list, not under V. Eq. 17 on line 670 is useful, but I suggest checking out eq. (15.69) on p. 533 of my book as well (after correcting the typos: the factor xˆ2 should not be there, and the factor us in both denominators should not be squared). This equation, as used by CALPUFF, gives predictions of final plume rise when both momentum and buoyancy affect plume rise.

The book reference is corrected and the alternate momentum equation has been added to the “conditions comparison” analysis.

Technical corrections.

All the technical corrections have been incorporated into the revised manuscript.

A Comparison of Plume Rise Algorithms to Stack Plume Measurements in the Athabasca Oil Sands

Mark Gordon[1], Paul A. Makar[2], Ralf M. Staebler[3], Junhua Zhang[2], Ayodeji Akingunola[2], Wanmin Gong[2], Shao-Meng Li[3]

1) Earth and Space Science and Engineering, York University
2) Air Quality Modelling and Integration Section, Air Quality Research Division, Atmospheric Science and Technology Directorate, Science and Technology Branch, Environment and Climate Change Canada.
3) Air Quality Processes Research Section, Air Quality Research Division, Atmospheric Science and Technology Directorate, Science and Technology Branch, Environment and Climate Change Canada.

Abstract

Plume rise parameterizations calculate the rise of pollutant plumes due to effluent buoyancy and exit momentum. Some form of these parameterizations is used by most air quality models. In this paper, the performance of the commonly used Briggs plume rise algorithm was extensively evaluated, through a comparison of the algorithm's results when driven by meteorological observations with direct observations of plume heights in the Athabasca oil sands region. The observations were carried out as part of the Canada-Alberta Joint Oil Sands Monitoring Plan in August and September of 2013. Wind and temperature data used to drive the algorithm were measured in the region of emissions from various platforms, including two meteorological towers, a radio-acoustic profiler, and a research aircraft. Other meteorological variables used to drive the algorithm include friction velocity, boundary-layer height, and the Obukhov length. Stack emissions and flow parameter information reported by Continuous Emissions Monitoring Systems (CEMS) were used to drive the plume rise algorithm. The calculated plume heights were then compared to interpolated aircraft SO_2 measurements, in order to evaluate the algorithm's prediction for plume rise. We demonstrate that the Briggs algorithm, when driven by ambient observations, significantly underestimated plume rise for these sources, with more than 50% of the predicted plume heights falling below half the observed values from this analysis. With the inclusion of the effects of effluent momentum, the choice of different forms of parameterizations, and the use of different stability classification systems, this essential finding remains unchanged. In all cases, approximately 50% or more of the predicted plume heights fall below half the observed values. These results are in contrast to numerous plume rise measurement studies published between 1968 and 1993. We note that the observations used to drive the algorithms imply the potential presence of significant spatial heterogeneity in meteorological conditions; we examine the potential impact of this heterogeneity in our companion paper (Akingunola et al, 2018). It is suggested that further study using long-term in-situ measurements with currently available technologies is warranted to investigate this discrepancy, and that wherever possible, driving meteorological observations are conducted in the immediate vicinity of the emitting stacks.

Commented [MG1]: New analysis looks at modifications to the original parameterization.

Commented [MG2]: There is an added focus on the effect of heterogeneity in the region, which is examined in the companion paper.

1. Introduction

In large scale air-quality models, grid cell sizes may be on the order of 1 km or larger, while vertical resolution may be in the tens to hundreds of meters (c.f. Makar *et al.*, 2015a,b). The large-scale impacts of transport by winds and turbulence are handled in these models by algorithms dealing with advection and turbulent diffusion of tracers. However, the redistribution of mass from elevated stacks with high-temperature and/or high-velocity emissions sources requires parameterization in order to deal with issues such as the buoyancy and momentum of the emitted mass. Briggs and others developed a system of parameterizations for plume rise beginning in the late 1960's (e.g. Briggs, 1969; Briggs, 1975). The parameterizations followed dimensional analysis to estimate plume rise based on meteorological measurements, atmospheric conditions, and stack parameters. Different variations of the Briggs plume rise parameterization equations are used in three-dimensional air-quality models such as GEM-MACH (Makar *et al.*, 2015a,b), CMAQ (Byun and Ching, 1999), CAMx (Emery *et al.*, 2010), as well as AEROPOL, SCREEN3, and CALGRID models (see Holmes and Morawska, 2006 for a summary of these models). The Briggs equations are also used in the Regional Acid Deposition Model (RADM, Byun and Binowski, 1991), and have been incorporated into emissions processing systems such as SMOKE (CMAS Website) and SMOKE-EU (Bieser *et al.*, 2011a).

As summarized by Briggs (1969), early observation of plume rise incorporated a wide variety of methods. Plumes were visually traced on Plexiglas screens, photographed, compared in height to nearby towers, and measured with lidar. Other techniques included the release of Geiger counters attached to balloons, and the release of balloons from within the stack chimneys. Bringfelt (1968) summarizes other techniques, using either theodolite, cloud height searchlights, or fluorescent particles sampled by aircraft-mounted instruments. Scaled wind tunnel simulations were also used. These observations were used to constrain the plume rise parameterizations and to choose appropriate constants following dimensional analysis (see Bieser *et al.*, 2011b for a summary).

Once a set of equations for plume rise had been developed, further observations were used to test their accuracy. A report of these comparisons (VDI, 1985) summarizes five studies in which plume rise parameterizations were compared to observations. These studies consistently show a tendency to overestimate plume rise using the Briggs parameterizations. Giebel (1979) measured pit coal power plant plumes with lidar which averaged 50% lower than the parameterization. Rittmann (1982) reanalyzed the Bringfelt (1968) and Briggs (1969) measurements from "industrial-sized sources" and found most plume heights were between 12 and 50% of the predicted rise. England *et al.* (1976) measured plume rise at a gas turbine facility with airborne measurements of NO_x and found plumes were 30% lower than predicted. Hamilton (1967) measured power station plumes with lidar which averaged 50% lower than the parameterization. Moore (1974) used data from seven locations measured with a variety of methods (photography, lidar, aircraft, and balloons) and found measured plume rise was 10-20% lower than the parameterization. The authors of the VDI (1985) report recommend reducing the plume height predicted by the Briggs equations by 30% during neutral conditions. No recommended adjustment for stable and unstable conditions was proposed, primarily due to a lack of supporting data. Sharf *et al.* (1993) measured the rise of power plant plumes with aircraft-based SO_2 measurements and found that plume heights were generally overestimated by the parameterization by up to 400 m. More recently, Webster and Thompson (2002) tested the Briggs equations as well as a more complex Lagrangian model using a network of surface concentration measurements downwind of a power plant. The Briggs algorithm resulted in concentration predictions which were biased high relative to observations, potentially indicating a tendency to underestimate plume rise, as emissions distributed over a lower vertical height would result in higher concentration. However, there may be other factors leading to the overestimation, such as poorly modelled winds or overestimated emission rates. Hence, the majority of earlier studies which have been compared to the original Briggs plume rise parameterization indicated some degree of overestimation of the actual plume rise, with a single more recent study possibly suggesting an underestimation of actual plume rise (inferred through surface measurements).

In the summer of 2013, as part of the Canada-Alberta Joint Oil Sands Monitoring (JOSM) Plan, aircraft measurements and monitoring stations were used to study dispersion and chemical processing of pollutants emitted from sources in the Athabasca oil sands region of northern Alberta. The GEM-MACH model (nested to 2.5 km resolution) was run from August through September, coincident with the measurement campaign, as an aid in directing aircraft flights and in subsequent post-campaign analysis of the observations. The model makes use of the Briggs plume rise algorithms. The large stacks in the region emit many key pollutants, such as SO_2, NO_x, VOCs, CO, and aerosols. The accuracy of the plume calculations thus has significant impact on model predictions, particularly close to the sources.

This manuscript evaluates the performance of the Briggs plume rise parameterization, as it is formulated in Environment and Climate Change Canada's GEM-MACH model, in a "stand-alone/off-line" sense, using meteorological observations as well as stack parameter data to drive the Briggs algorithms. For comparison, another model proposed by Briggs (1984) for irregular stability profiles is also evaluated. We also make use of aircraft observations of emitted SO_2 in order to evaluate the accuracy of the algorithms.

In our companion paper (Akingunola *et al.* 2018, this issue) we examine the potential impact of the observed heterogeneity in meteorological data on plume rise predictions, comparing high resolution GEM-MACH plume locations to aircraft observations, as well as the effects of different sources of stack data on simulated plume rise performance.

2. Methods

2.1 Plume Rise Parameterization in GEM-MACH.

The plume rise (Δh) calculation in GEM-MACH is driven by 9 variables: stack height (h_s), exit temperature at the stack outlet (T_s), stack emission volumetric flow rate (V), air temperature at stack height (T_a), wind speed at stack height (U), surface temperature ($T_{surface}$), boundary-layer height (H), friction velocity (u_*), and Obukhov length (L). These input parameters are used to generate the rise in the plume above the stack height (Δh), as well as the upper and lower boundaries of the plume having risen to equilibrium. In models such as GEM-MACH, buoyant transport of emissions through that region is assumed to be instantaneous. The emitted mass is distributed through the given region under the assumption that the buoyant plume has reached equilibrium. Here, all of these variables are obtained from observations (either directly or via the use of the appropriate formulae with observed quantities).

The algorithm makes use of derived quantities (the buoyancy flux, F_b, the stability parameter, s, and the convective velocity, H_*) with different formula for plume rise corresponding to *neutral*, *stable*, and *unstable* atmospheric conditions. The buoyancy flux is calculated from Briggs (1984, equivalent to their Eq. 8.35) as

$$F_b = \begin{cases} \frac{g}{\pi} V \frac{(T_s - T_a)}{T_s}, & T_s > T_a \\ 0, & T_s \leq T_a \end{cases}, \tag{1}$$

where $g = 9.81$ m s^{-2} is the gravitational acceleration. The stability parameter is calculated from Briggs (1984, combining their Eq. 8.8 and Eq. 8.14) as

$$s = \frac{g}{T_a}\left(\frac{dT_a}{dz} + \frac{g}{c_p}\right). \tag{2}$$

where z is the height coordinate and $c_p = 1005$ J K^{-1} kg^{-1}. The temperature gradient is calculated from the temperature difference over the stack-height ($dT/dz = \left(T_a - T_{surface}\right)/h_s$), with a minimum value set at –5 K/km (i.e. $s \geq 0.047/T_a$). We note that calculating the temperature difference between the stack height and the surface may underestimate the temperature gradient above the stack height, where the plume rises. The extent of this effect is tested later using temperature gradients throughout the boundary layer (Section 2.2). Finally, the convective velocity ($H_* = -2.5 u_*^3/L$) is defined in Briggs (1985).

Commented [MG3]: Corrected from "maximum" and text added for clarity.

The plume is considered *neutral* if $L > 2h_s$ or $L < -0.25h_s$ (i.e. $-4 < \frac{h_s}{L} < 0.5$). These values are suggested in Briggs (1984) and the sensitivity of the results to these values is tested in Section 4. The plume rise in neutral conditions is taken as the minimum of two formulations of Briggs outlined in Sharf *et al.* (1993) and Byun and Ching (1999) as

$$\Delta h = \min\left[39\frac{F_b^{3/5}}{U} \ , \ 1.2\left(\frac{F_b}{u_*^2 U}\right)^{3/5}\left(h_s + 1.3\frac{F_b}{u_*^2 U}\right)^{2/5}\right]. \tag{3}$$

The atmosphere is considered *stable* at the plume height if either $0 < L < 2h_s$ (stable conditions) or $h_s \geq H$ (direct emission above the boundary-layer). From Briggs (1984, their Eq. 8.71), the plume rise is calculated as

$$\Delta h = 2.6\left(\frac{F_b}{sU}\right)^{\frac{1}{3}}. \tag{4}$$

The atmosphere is considered *unstable* if $-0.25h_s < L < 0$. In the unstable case, the plume rise is taken as the minimum value of two formulations of Briggs outlined in Byun and Ching (1999),

$$\Delta h = \min\left[3\left(\frac{F_b}{U}\right)^{\frac{3}{5}} H_*^{-\frac{2}{5}}\ ,\ \ 30\left(\frac{F_b}{U}\right)^{\frac{3}{5}}\right]. \tag{5}$$

This effectively places a lower limit on the magnitude of the convective velocity in determining plume rise as $H_* > 0.00316$ m^2/s^3 (from $H_*^{-2/5} < 10$). Briggs (1984) gives the example of clear summer conditions as $H_* = 0.007$ m^2/s^3.

The only difference between Eqns. 3, 4, and 5 and the plume rise parameterizations used in SMOKE (described in Bieser *et al.*, 2011 and Houyoux, 1998) is the option of the minimum values in unstable and neutral conditions. In the SMOKE model, only the second parameterizations within the minima of Eqns. 3 and 5 are used. Both the approaches used in GEM-MACH and SMOKE are investigated in the following analysis.

Plume rise is also modified for situations where the stack height is less than the boundary-layer height ($h_s < H$), but the plume rises high enough to penetrate the boundary-layer height to some degree ($h_s + \Delta h > H$). This is referred to as "bumping" (Briggs, 1984). The vertical plume depth is assumed to be equal to the plume rise so that the plume is bound by the height range $h_s + 0.5\Delta h < z < h_s + 1.5\Delta h$. If any portion of the plume is above H, the plume rise is calculated (from Briggs, 1984) as

$$\Delta h = (0.62 + 0.38p)(H - h_s), \tag{6}$$

where p is the fraction of the plume above H (i.e. $p = 0$ if $h_s + 1.5\Delta h = H$ and $p = 1$ if $h_s + 0.5\Delta h = H$).

While the above formulae are used in GEM-MACH and other models, we also examine a layer-based approach suggested by Briggs, described below, and the companion paper, Akingunola *et al.* (2018), examines the impact of this approach within the GEM-MACH model itself.

2.2 Plume Rise into Irregular Stability Profiles (The Layered Method)

In addition to the parameterization discussed above, Briggs (1984) suggests a layer-based approach to calculate plume rise for complex stability profiles. In this approach, the plume buoyancy (F) is modified as it passes through each discrete layer as

$$F = F_j - 0.053 s_j U_j \left(z_c^3 - z_j^3\right) \tag{7}$$

where F_j is the buoyancy flux at the bottom of layer j, s_j is the layer stability calculated using Eq. (2), U_j is the wind speed, and z_j is the layer height above the stack height. The wind speed in the original Briggs formulation is taken as constant with height, while here we use an average wind speed for each layer. The lower boundary of the first layer is the stack height $(z_{j=0} = 0)$. The value of F is determined sequentially for each layer at the top of each layer (with $z_c = z_{j+1}$) until it becomes negative. For the layer where F becomes negative, Eq. 7 is solved to give the plume height z_c for which $F = 0$. Plume rise is calculated as $\Delta h = z_c$. Layer thickness will depend on the vertical model or measurement resolution. Layer thickness for this analysis is discussed in detail in Section 2.6.

Commented [MG4]: The lower boundary was given as hs (stack height) in the previous manuscript. This is corrected.

Equation 7 is intended for use with stable ($s > 0$) or neutral ($s = 0$) layers. For unstable layers we follow the approach outlined in our companion paper (Akingunola et al., 2018) in which the plume rises through the unstable layer without gaining or losing buoyancy or momentum (equivalent to $s = 0$ in Eq. 7). As is discussed below (Section 4.1), the majority of layer temperature profiles (>90%) measured by the aircraft were stable or neutral, so this assumption should not have a significant effect on the resulting plume rise. However, we also hound that the stability was spatially heterogeneous in the study region, with significant differences in stability noted from the different sources of meteorological information.

Commented [MG5]: An added discussion of how the model handles unstable profiles and the effect this might have on the results.

While the Briggs parameterization discussed in Section 2.1 is driven by surface (or near-surface) observations, the layered method (Eq. 7) is driven by observations up to the height of the plume. The observed plume centreline heights (Section 2.7) vary between approximately 100 m and 1000 m above the surface. Hence the layered method can be used with the elevated observations from an aircraft measurement platform and an acoustic profiler (Section 2.4).

2.3 Stack Height (h_s), Exhaust Temperature (T_s), and Flow Rate (V)

Commented [MG6]: This section is modified to make it clear than only the flaring stack (CNRL2) uses NPRI data. All other stacks are driven by CEMS hourly data.

As part of the Continuous Emission Monitoring System (see CEMS, 1998), measurements of 19 stacks in the region of study with valid hourly measurements of SO_2 and average effluent velocity and temperature were obtained from Alberta Environment and Parks. Stacks which emit primarily NO_x and no reported SO_2 are not used in this analysis. A key requirement for our evaluation is that the stacks selected for comparison have sufficient levels of SO_2 emissions to be easily discernable from the aircraft observations. For stacks without reported CEMS SO_2 emission rates, the average rates determined from the Cumulative Environmental Management Association inventory for the year 2010 (see CEMA, 2012) were used to eliminate stacks from the analysis which would not emit enough SO_2 to be observed by the aircraft-based instrumentation. It is assumed that the emission profiles of SO_2 in 2013 are not significantly different from 2010. Stacks from the Imperial Oil Kearl facility are not in the CEMA inventory because those stacks started operation later than 2010. A comparison of observed plume locations, as outlined below in Section 2.7, demonstrates that the Kearl and Firebag stacks produce no discernable SO_2 plumes. Based on this comparison, there are 7 stacks which emit significant (more than 0.050 kg s^{-1}) SO_2. The 12 non-SO_2 emitting stacks all report less than 0.005 kg s^{-1}.

A flaring stack at the CNRL facility was added to the list (CNRL2) because daily reports indicated a large amount of SO_2 emissions were released from the flaring stacks for a one-week period during the field study. However, by their nature (a high temperature flame at the top of the stack is used to loft pollutants upwards), CEMS monitoring of flare stacks is not possible with current technology, and hence emissions rates and stack parameters for this source are engineering estimates. The stack parameters for this flaring stack were parameterized using effluent velocity and temperature based on annual NPRI inventory values (NPRI ID 23275; NPRI Website, see ECCC & AEP, 2016).

Although NRPI data are available for the CNRL flaring stack, the other CNRL stack used here (a "sulphur recovery unit") has both CEMS and NPRI data available. This allows for a test of the variability in T_s and w_s through comparison of NPRI data (where annual average values are reported) and CEMS data (hourly) for this period and stack. For stack CNRL1 the annual average NPRI values were $T_s = 811$ K and $w_s = 17$ m s^{-1}, and the CEMS data averages for the study period are $T_s = 851$ K and $w_s = 4.1$ m s^{-1} (a 5% temperature difference and more than a factor of 4 difference in flow rate). Hence there may be significant differences between data reported through both methods; by extension the CNRL2 values (for the one-week period it is active) should be considered only approximations.

Commented [MG7]: A comparison to another stack is added to estimate the uncertainty in the NPRI estimated parameters.

All 8 stacks are listed in Table 1 and the locations of these 8 stacks are shown in Fig. 1. For comparison, average effluent velocities (calculated from flow rate and stack diameter as $w_s = 4V/\pi d_s^2$) and temperatures were calculated for each stack over the 84 hours of research aircraft flight time (with the exception of CNRL2, which is based on annual NPRI inventory values). These averages are shown for comparison only; plume rise in the analysis which follows is calculated using hourly CEMS data concurrent with the time of plume observations. Plume observations and the aircraft flight campaign are discussed in more detail in the following sections.

Commented [MG8]: Stacks which do not emit significant SO2 are not used in the analysis and have been removed from Table 1.

Table 1. CEMS stack parameters for all stacks within flight area which emit significant SO_2, including location and elevation at the stack base ($z_{surface}$), stack height (h_s), stack diameter (d_s), effluent velocity at the stack exit (w_s), and effluent temperature at the stack exit (T_s). Velocities and temperatures shown here are averages for the entire flight period. Hourly CEMS values are used for plume rise calculations. Stack numbers (#) are for identification within this analysis and do not represent official reporting ID. The SO_2 emission rates from 2010 inventory are shown for comparison.

Facility	#	Latitude	Longitude	$z_{surface}$ [m amsl]	h_s [m]	d_s [m]	w_s[m/s]	T_s [K]	SO_2 [kg/s]
Suncor	1	57.0020	-111.4770	257	106.7	5.8	<0.1	404.3	0.14
Suncor	2	57.0050	-111.4770	254	106.7	2.0	9.3	711.5	0.06
Suncor	3	57.0030	-111.4770	256	137.2	7.0	<0.1	336.3	0.19
Suncor	4	57.0060	-111.4790	255	106.1	3.4	4.2	947.3	0.17
Syncrude	1	57.0410	-111.6160	304	183.0	7.9	12.0	472.9	2.27
Syncrude	2	57.0480	-111.6130	305	76.2	6.6	10.1	350.7	0.12
CNRL	1	57.3390	-111.7380	284	106.7	3.4	4.1	851.1	0.20
CNRL*	2	57.3390	-111.7380	284	109.0	1.4	6.2	1273.1	N/A*

* The CNRL#2 flaring stack is added based on NPRI inventory and is assumed to emit significant SO_2 for a 1-week period during the field study.

The relatively high flow rates and diameters of some stacks may lead to plume rise due to momentum alone, especially under stable conditions. Briggs also developed similar equations for rise due to momentum (c.f. Briggs, 1984). These equations are typically used when $F_b = 0$, and the plume is assumed to be either a vertical jet (momentum driven) or a bent over plume (buoyancy driven). The potential effect of momentum on the plume rise is discussed in Section 4.4.

Commented [MG9]: There was an brief analysis of rise due to momentum here. This analysis is done later in Section 4.4.4.

2.4 Measurement Platforms

Wind speed (U), wind direction (θ), and temperature (T_a) data at the stack height and at the surface were estimated based on measurements made at either: one of two meteorological towers in the study region (WBEA: AMS03 and AMS05); or a radio-acoustic sounding system (*wind*RASS, Scintec). Figure 1 demonstrates the sites of the WBEA meteorological towers, and the radio-acoustic sounding system (RASS).

Commented [MG10]: The scale in image (b) is corrected from 50 km" to "20 km".

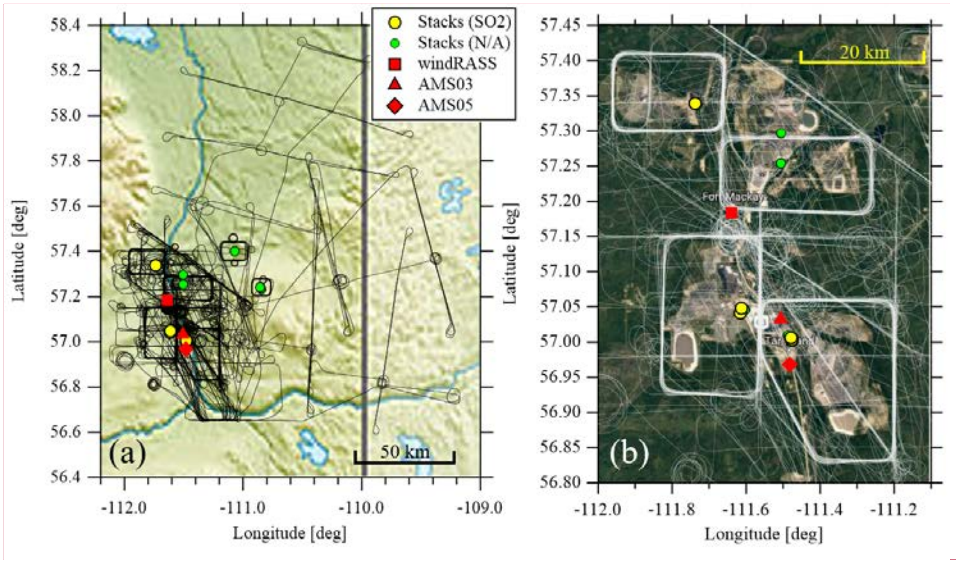

Figure 1. The flight tracks (black lines on (a), white lines on (b)) during the 22 flights of the JOSM study, compared to the location of: the facility stacks, including SO_2 emitting stacks used for this analysis (yellow circles) and non-SO_2 emitting stacks (green circles); the radio-acoustic profiler (windRASS, red square); and the WBEA meteorological towers, AMS03 (red triangle); and AMS05 (red diamond). Stack towers in close proximity are overlapping. The relief map (a) shows the extent of the flight area and the Athabasca river valley with the Alberta/Saskatchewan border shown at –110° longitude (Wikipedia, credit: Carport). The satellite image (b) is a close up in the region of the facilities (Google: Landsat/Copernicus, 2017).

The AMS03 tower measures wind speed, wind direction and temperature at heights of 20, 45, 100, and 167 m (all heights above ground level). The AMS05 tower measures wind speed and direction at heights of 20, 45, 75, and 90 m and temperature at heights of 2, 20, 45, and 75 m. Tower measurements are reported as 1-hour averages. The RASS measures wind speed and temperature (among other variables) between a minimum height of 40 m and a maximum height which varies depending on wind conditions (Cuxart *et al.*, 2012). During the aircraft flight period, the maximum RASS measurement height varied from 130 m to 800 m, with an average 336 m. The RASS measurements are 15-min averages.

As part of JOSM, aircraft-based measurements were made in the Athabasca oil sands region between August 13 and September 7, 2013. The project included 22 flights, which were flown in some combination of either box formations (circumnavigating a facility at variable heights in order to determine facility pollutant emissions), screen formations (flown perpendicular to the plume centreline axis to characterize the transformation of the plumes), spiral ascent and descent (to characterize boundary-layer structure), or horizontal area coverage (to verify satellite observations over a larger spatial extent). Figure 1 shows all these flight formations. Within the 22 flights, there were 16 box-flight formations and 21 screens used for this analysis. Aircraft flight times varied from approximately 2.5 hours to over 5 hours, typically in the mid-afternoon, for a total of 84 hours. Wind speeds and temperatures were measured from the aircraft with a Rosemount 858 probe, sampled at 32 Hz and averaged to 1 Hz. For details of the aircraft measurements, see Li *et al.* (2017), Liggio *et al.* (2016), and Gordon *et al.* (2015). The aircraft flew at a minimum height of 150 m above ground level (agl). The maximum height of box formations varied from 500 m agl to 1300 m agl, while the maximum height of screen formations ranged from 350 m agl to 2000 m agl.

Table 2. Correlation coefficient (R^2) of wind speeds (U), wind directions (Ψ), and temperature (T) at given comparison heights.

		Comparison Height	R^2		
			U	Ψ	T
RASS	AMS03	167 m	0.61	0.88	0.84
AMS03	AMS05	90 m	0.80	0.94	0.98
AMS05	RASS	90 m	0.56	0.84	0.82
Aircraft	RASS	< 200 m	0.66	0.60	0.82
Aircraft	AMS03	< 200 m	0.61	0.63	0.78

Tower, RASS, and aircraft measurements were compared over the 84 flight hours. The RASS was not operational until Aug. 17 (thus missing 3 flights); hence RASS data are compared for a reduced period. For comparison to the tower measurements, the 15-min RASS and 1-s aircraft measurements were averaged to concurrent 1-hour values. For comparison to the RASS, the 1-s aircraft measurements were averaged to 15-min values. The resulting correlation coefficients are listed in Table 2. The aircraft wind and temperature measurements are also compared with the highest tower (AMS03) and the RASS. For comparison to aircraft measurements, the RASS measurements at a height of 90 m were compared to all concurrent aircraft measurements below 200 m. In the case of AMS03, the measurement at a height of 167 m was compared to all concurrent aircraft measurements below 200 m. The wind speed comparisons are best between the two towers ($R^2 = 0.80$). Wind direction compares well for the towers and the RASS ($R^2 > 0.84$). Temperature compares well for all measurement platforms ($R^2 > 0.78$). Generally, comparisons with the aircraft give the lowest correlation values. We note that the correlations of Table 2 do not show potential local offsets in magnitude, and that the aircraft observations are averages over a larger region which may not be spatially co-located with the towers. We also note from Figure 1(b) that towers AMS03 and AMS05 are less than 10 km apart, while the RASS is approximately 20 km from the two towers. The correlations between AMS03 and AMS05 are higher than between either of these towers and the more distant RASS, and that correlations with the aircraft have the lowest values, implying that some of the lower correlations may reflect local heterogeneity in meteorological conditions.

We note that the Athabasca oil sands region is centered on the Athabasca River valley, with over 500m of vertical relief within 60 km of the facilities; the flow within the valley may be complex, with frequent observations of shear between plumes from stacks at different elevations under stable conditions. The low correlations between the stations and between the stations and the aircraft reflect this variation in local meteorological conditions. We examine this possibility through the use of a high resolution GEM-MACH simulation in our companion paper (Akingunola et al, 2018).

2.5 Stability (z/L), Boundary-Layer Height (H), and Friction Velocity (u_*)

Stability, boundary-layer height, and friction velocity were all determined from the observations using wind speed and temperature profiles from multiple height measurements. The towers, which have anemometers and temperature sensors at variable heights between 2 m and 167 m, measured within the surface layer and are best suited for these estimations. The RASS, which has a minimum measurement height of 40 m, may not capture the surface layer effectively. As the aircraft did not fly below a height of 150 m, aircraft-based measurements cannot be used to estimate the stability, boundary-layer height, and friction velocity. For our analysis, we calculate L, H, and u_* to drive the Briggs parameterization (Eqns. 1-6) using observations from the two towers (AMS03 and AMS05) and the RASS.

The atmospheric stability is determined using the Bulk Richardson Number, which is defined (Garratt, 1994) as

$$R_i = \frac{g z_h}{\theta} \frac{\Delta\theta}{\Delta U^2}. \tag{8}$$

Commented [MG11]: Equations 8 and 10 are modified to use potential temperature.

Here $\Delta\theta$ and ΔU are the potential temperature and wind speed differences over the height range (z_h). The height range is determined as the difference in height between the highest measurement location and the lower measurement location. For example, z_h =147 m for AMS03, $z_h = 55$ m for AMS05, and z_h is variable for the RASS. The Richardson number is then related to the stability parameter (Kaimal and Finnigan, 1994) as

$$\frac{z}{L} = \begin{cases} R_i & \text{for } R_i < 0 \\ \dfrac{R_i}{1 - R_i/R_{ic}} & \text{for } 0 < R_i < R_{ic} \\ +\infty & \text{for } R_i > R_{ic} \end{cases} \tag{9}$$

Here $R_{ic} = 0.25$ is the critical Richardson number, chosen as the mid-range of reported values (0.2, 0.25, or 0.5; Mahrt, 1981). For $R_i > R_{ic}$ there is no solution, so this is modelled as extremely stable boundary-layer with L slightly larger than zero (to satisfy the stability condition $L > 0$). The Obukhov length is calculated from the stability parameter as $L = z_{max}/(z/L)$, where z_{max} is the highest measurement height of 167 m, 90 m, or up to 800 m for AMS03, AMS05, and the RASS respectively.

Boundary-layer height can be parameterized for stable and unstable conditions following Mahrt (1981) as

$$H = \frac{R_i T_{sur}}{g} \frac{U(H)^2}{\theta(H) - \theta_{surface}}, \tag{10}$$

where R_i is the bulk Richardson number and $U(H)$ and $\theta(H)$ are the respective wind speed and potential temperature at the boundary-layer height and $\theta_{surface}$ is the potential temperature at the surface. Since measurements at the boundary layer height may not be available, we approximate the wind speed to temperature gradient ratio in Eq. 10 as $U(z_{max})^2/\big(\theta(z_{max}) - \theta_{surface}\big)$.

The boundary-layer height derived from Eq. 10 can be compared to the boundary-layer height estimated from in-situ aircraft measurements of the CH_4 mixing ratio during vertical profile flight formations. These CH_4 profiles demonstrate a well-defined background level above a given height, with elevated CH_4 mixing ratios below this height. The boundary-layer heights determined by the aircraft measurements range from 340 m to 1790 m with an average of 1180 m. The values of H derived from Eq. 10 using the AMS03 tower data for the same time periods as the flights range from 460 m to 3050 m, with an average of 1160 m.

The friction velocity (u_*) was determined from the wind speed profile (Garratt, 1994) as

$$u(z) = \frac{u_*}{k}\left[\ln\left(\frac{z}{z_o}\right) - \Phi\right], \tag{11}$$

where z_o is the roughness length, $k = 0.4$, and the stability parameter is

$$\Phi = \begin{cases} 2\ln\left(\frac{1}{2}(1 + x_o)\right) + \ln\left(\frac{1}{2}(1 + x_o^2)\right) - 2\,\mathrm{atan}(x_o) + \frac{\pi}{2}, & \text{for } \frac{z}{L} < 0 \\ -5\frac{z}{L} & \text{for } \frac{z}{L} > 0 \end{cases} \tag{12}$$

with $x_o = (1 - 16z/L)^{1/4}$. A least-squares method is used for each hourly profile to determine an appropriate z_o for the measurement location, which is taken as the median value of all the hourly fits. This median z_o value calculated using this method varies considerably by location (1.5m for AMS03, 0.75 m for AMS05, 10.1 m for RASS). The median z_o values were then used to calculate u_* using the hourly wind speed measured at the highest location. The calculation of u_* with the RASS may be inaccurate due to the lack of measurements between the surface and a height of 40 m. However, the large difference in values of z_o may be also due to the different environment surrounding the measurement locations, since the towers are surrounded by forest and the RASS is located in the town of Fort McKay.

It is noted that parameterizing stability without a measurement of heat flux and estimating boundary-layer height based on near surface measurements may lead to significant uncertainties in these values. This will also affect the estimation of u_*, and may be evident in the median z_o values for the RASS, which are very large even for a town with 2 or 3-story buildings. Tests to determine the sensitivity of the calculated plume rise to these variables (L, H, u_*) are discussed in Section 4.2.

Commented [MG12]: Some discussion of the limitations of this method (to estimate L and H) is added.

2.6 Stability Profile Measurements for the Layered Method

To drive the layered method discussed in Section 2.2, profiles of temperature and wind speed were derived for each box and each screen using RASS and aircraft observations. RASS layers were 10 m thick to match the instruments resolution. The lowest RASS measurement is at a height of 40 m, well below the lowest stack height (76 m). Because the maximum observation height of the RASS varies (with an average of 336 m), it was necessary to extrapolate temperature and wind speed above the maximum measurement height in some cases. This was done by assuming a constant wind speed and a constant temperature gradient, based on measurements in the highest 100 m of observations.

For aircraft observations, the box and screen flights were designed to approximate 100 m vertical spacing between each box circuit or screen pass. Based on this resolution we use a layer thickness of 100 m for the layered method driven by aircraft observations. Testing demonstrates that the algorithm is not sensitive to the layer thickness. Flight measurements of wind (U) and temperature (T) for each box and screen are averaged in vertical layers within the 100 m spacing. Since there are no measurements below a height of 150 m agl, the temperature at the lowest layer ($0 < z < 100$ m) is extrapolated by assuming a constant lapse rate and stability below 200 m (i.e. $s_{j=1} = s_{j=0}$). There are no cases of calculated plume height based on the layered method exceeding the maximum aircraft measurement height and hence no need for upward extrapolation of the measurements.

Our temperature profiles for the layered method thus have as key assumptions: (1) that the profiles at the RASS location and derived from the aircraft are representative of conditions at the stacks, and (2) that the extrapolations and vertical resolution used here provide a reasonable representation of the atmospheric temperature profile .

Commented [MG13]: Added caveat for heterogeneity in the region.

2.7 Measured Plume Heights and Stack to Plume Matching Algorithm

The aircraft measured numerous pollutants, of which SO_2 is used here to define the stack plume locations since approximately 95% of the SO_2 emissions in the region originate in stacks (Zhang *et al.*, this issue). The SO_2 analyzer (Thermo Fisher Scientific, model 43i) on the aircraft measured at a rate of 1 Hz. The flight paths were designed to create a 100 m spacing between measurement points (in both horizontal, s, and vertical, z) in order to optimize interpolation of the measurements. The measurements were interpolated in s and z using simple kriging as outlined in the Topdown Emission Rate Retrieval Algorithm (TERRA; Gordon *et al.*, 2015). This creates two-dimensional images of SO_2 mixing ratio. For box flights, which circumnavigate the facilities, the s coordinate is the distance along the box in the counter-clockwise direction from the southeast corner. For screens, s is the lateral distance along the screen, generally perpendicular to the wind direction. Below the lowest flight path (at 150 m agl), no interpolation is performed and the screen is left blank between this level and the ground. Figures 2 and 3 show example box and screen flight paths in both horizontal (Fig. 2) and vertical (Fig. 3) profiles.

A semi-empirical approach was used to match each stack to the observed plume locations. The wind direction measured from the aircraft was averaged for the duration of each box or screen. Tower or RASS-based wind direction measurements were not used, as an initial comparison of wind directions and observed plume locations demonstrated that the aircraft measurements are a better representation of the wind direction associated with plume transport than surface measurements. This agreement is most likely due to the consistent proximity of the aircraft to the stack sources; the towers and RASS locations can often be much further away (Fig. 1).

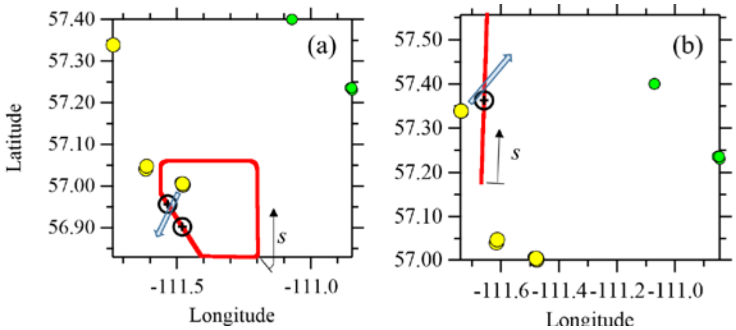

Figure 2. Example horizontal flight path of a box flight (a) and a screen flight (b). Flight paths for the box and screen portion of the flight shown as red lines. Stack locations are shown as filled yellow circles (SO_2 emitting) and green circles (non-SO_2 emitting). The blue arrow shows the forward trajectory of the plume using the average wind direction during each flight segment. The plume locations determined by observations (Fig. 3) are shown as black cross-hairs on the flight paths. The location of the flight path coordinate s origin is labeled in each figure.

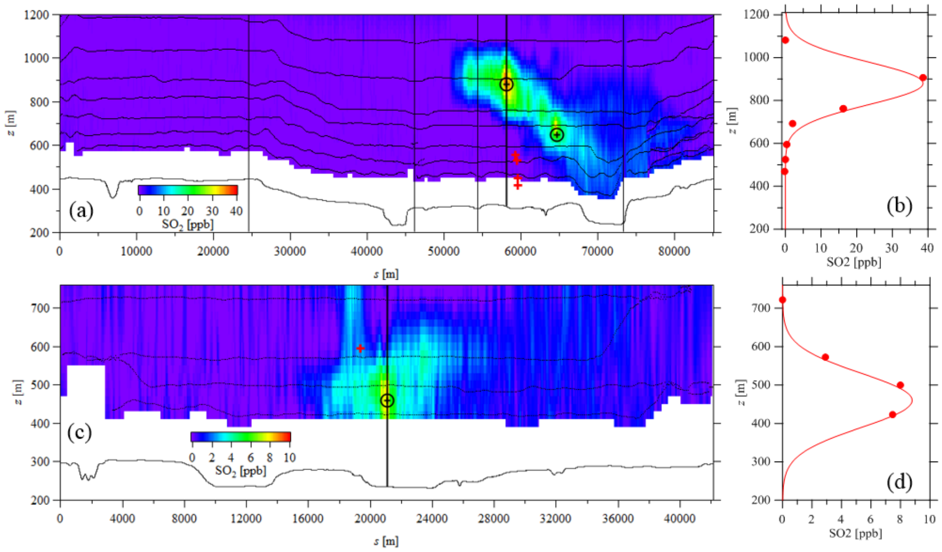

Figure 3. The interpolated images for the box flight (a) and the screen flight (c) (as Fig. 2). The aircraft flight paths are marked by the finely spaced (1 Hz) black dots. The surface location ($z_{surface}$) is shown below the flight path. Interpolation is removed between the lowest flight path and the surface, following the TERRA method. In the box (a), the thin vertical lines show the box corners (see Fig. 2a). The plume locations determined by the Briggs plume rise and the forward trajectories (s_{int}, z_h) are marked by red plus signs. The plume locations determined by observations (s_p, z_p) are shown as black cross-hairs. The Gaussian fitting used to improve plume height estimation is demonstrated (b,d) for the location marked by the thick vertical black line in each image.

The average wind directions were then used to predict the direction of plume transport downwind of each stack. The intercept of each plume's predicted path with the box or screen (s_{int}) was calculated based on this forward trajectory from the stack source to the box or screen intercept. Example box and screen flight paths, forward trajectories, and observed plume locations are shown in Figure 2 for the flights on Aug. 29 (Fig. 2a) and Aug. 15 (Fig. 2b). This simple forward trajectory methodology ignores the local effects of topography, vertical winds, and the variability of the wind during the box or screen segment of each flight (typically less than 2 hours of flight time). Some screens were flown up to 150 km from the 8 stacks (see Fig. 1). Since other stratification, topography, and diffusion effects may influence a plume height at such a large distance from the plume origin, we restrict our analysis to box walls and screens within 50 km of the plume stack sources.

Plume rise (Δh) was calculated for each stack based on the Briggs parameterization, the observed meteorological conditions at the tower or RASS locations (or RASS and aircraft data, for the layered approach), and the CEMS stack parameters, all averaged for the duration of the box or screen flight periods. This calculation also defined the estimated plume centreline location at each box or screen as (s_{int}, z_h), where $z_h = z_{surface} + h_s + \Delta h$ and $z_{surface}$ is the surface elevation (amsl) at the intercept.

The flight path observations are converted to two-dimensional (s, z) images by kriging interpolation following the method outlined in Gordon *et al.* (2015). Example interpolated images from both a box and a screen flight are shown in Figure 3. A disadvantage of kriging interpolation of the aircraft data is that the maxima of the plumes will always be fixed at a flight measurement location. To improve the resolution of observed plume height from the interpolated images, the aircraft measurements within a 100-m wide window (i.e. s ± 50m) are fitted to a Gaussian vertical profile. Example profiles are shown in Figures 3b and 3d, which correspond to the windows shown as thick black lines through the maximum SO_2 locations (the plume centres) in Figures 3a and 3c. The maxima of the Gaussian fits for each identified plume are then used to identify the prominent plume locations as (s_p, z_p). The identified plume locations are visually compared to the predicted Briggs plume locations based on the forward trajectories for each box or screen (s_{int}, z_h).

Stationarity of the wind speed, wind direction, and plume buoyancy during the measurements is a potential source of uncertainty as each flight circuit (or pass) around the facility can take between 10 and 15 minutes. This effect is discussed in Gordon et al. (2015) for this flight campaign. Although this can have significant effect on the calculation of emissions, the effect on the estimation of plume height should be less than the vertical distance between passes (~100 m). Further, some flights were flown from bottom to top, while others were from top to bottom, so there should be no directional bias on average.

Each calculated plume location (s_{int}, z_h) was paired with each nearby observed plume location (s_p, z_p) to maximize the correlation of calculated and observed plume heights. For example, the calculated plume rise from three stacks would be paired with three observed plume heights by matching the lowest calculated plume height to the lower observed plume height; the middle calculated plume height to the middle observed plume height; and the highest calculated plume height to the highest observed plume height. This gave the highest correlation between predicted values and observations. For a single plume observation and multiple SO_2-emitting upwind stacks, the stack plumes were assumed to have merged and the calculated plume height for each stack was paired to the same observed plume height. The merging of plumes is supported by visual observation by the authors during the field study, especially far downwind of the stack locations.

For the example of the Aug. 15 screen flight (Fig. 2b and Figs. 3c,d), the forward trajectory and Briggs algorithm model intercept the flight screen approximately 2 km further south, and 140 m higher, than the observed plume centre, indicating the possibility of more complex wind flow than a simple trajectory. In the example of the Aug. 29 box flight (Fig. 2a and Fig. 3a,b), there are two observed plumes along the NW-SE oriented wall of the box. The forward trajectory model places the plume intercept between these two plumes, closer to the vertically higher and more northern observed plume at the horizontal location given by s = 58 km. There are four stacks within the box, two of which have calculated intercept heights near $z_h = 540$ m and two of which have calculated intercept heights near $z_h = 430$ m. All four calculated values are clearly well below the observed intercept heights (z_p = 650 m and 880 m). This demonstrates some ambiguity and subjectivity in this analysis, as four calculated plume locations must be matched to two observed plumes. As described above and for the purposes of statistical comparisons, we match the highest two modeled plumes (near heights of 540 m) with the highest observed plume (880 m) and the lower two modeled plumes (near heights of 430 m) with the lower observed plume (650 m).

3. Results

Commented [MG14]: All numerical results below have changed numerically due to the change to potential temperature for Eqns. 8 and 10. The conclusions (underestimation of plume rise by the algorithms) do not change for these corrected values.

3.1 Comparison of Measurement Platforms

The topography of the Athabasca oil sands region can be generally described as a north-south river valley approximately 1 to 5 km in width, within a larger and more gradually sloped north-south valley between 10 and 50 km in width, and up to 500 m of vertical relief (Fig. 1a). Local surface wind patterns can be heterogeneous, especially within the valley. The AMS03 and AMS05 towers are in the vicinity of the Suncor stacks and the Syncrude stacks (Table 1), while the RASS is nearly equidistant to the 8 stacks used for this analysis (Fig. 1b).

As an approximate measure of the uncertainty associated with local meteorology, plume rise values from the 8 stacks are compared using the Briggs parameterization (Eqs. 1-6) with all 3 meteorological measurement platforms (i.e. AMS03, AMS05, and RASS) as well using the layered method (Eq. 7) with both RASS and aircraft measurements. This comparison was done for all concurrent times during which the aircraft was flying box or screen patterns. There were approximately 26 hours during which the aircraft flew in a box pattern and 20 hours during which the aircraft flew in a screen formation, for a total of more than 46 hours. The resulting distributions of calculated plume heights for these 46 hours of flight time for the 8 stacks are compared in Figure 4.

The distributions of plume rise heights are similar for the Briggs parameterization with the three fixed, near-surface measurement platforms. Approximately 90% of the plume rise values calculated with the AMS tower and RASS measurements are below approximately 250 m, with half or more below 75 m. With the layered method, the plume heights calculated with the RASS measurements are similar to those calculated with aircraft measurements. As with the Briggs parameterization, approximately 90% of the plume rise values are below 250 m; however, more than half of the plume rise heights calculated with the layered method are above 125 m.

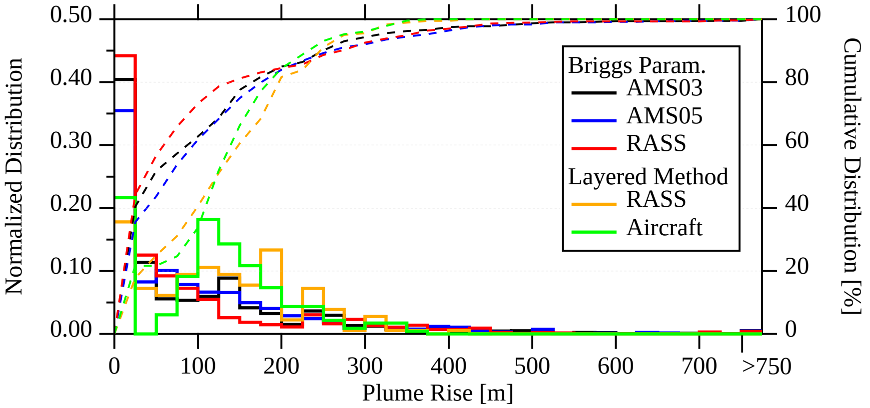

Figure 4. The distribution of calculated plume rise (Δh) using Briggs parameterization (Eqns. 1-6) with input data from the AMS03 and AMS05 towers and the RASS profiler, and the layered method (Eq. 7) with input date from the RASS profiler and the aircraft. Distributions are shown for each hour (using the 46 hours of box and screen flight times) and for all of 8 SO_2 emitting stacks combined. The right-most histogram bin is the sum of all values of $\Delta h > 750$ m. Cumulative distributions shown by dashed lines.

3.2 Predicted Plume Rise

The plume rise was calculated for each flight for each stack with the Briggs parameterization for each input (towers, RASS) as well as with the layered method (RASS, aircraft). These plume rises were then paired with the measured plume locations following the method described in Section 2.7. For simplicity, the parameterized plume rise is described as $h_B = \Delta h$, and the observed plume rise is described as $h_M = z_p - z_{surface} - h_s$. Results of this comparison are shown in Figure 5. The analysis resulted in 82 stack-to-observed plume pairings, for each measurement platform. (Note that a smaller number of pairings were possible for the RASS, which was not in operation for 4 of the 22 flight days). Table 3 compares the results for each measurement method. The low slopes (b <0.5), significant intercepts ($44 < a <$ 107 m), and low correlation coefficients ($r^2 \leq 0.2$) demonstrate that the Briggs parameterization of plume rise was a poor predictor of actual plume rise. For a 95% confidence (calculated from the standard error of the slopes) none of these slopes is significantly different from zero.

Using the tower or RASS measurements with the standard Briggs parameterization suggests an average underestimation (based on the average ratio) between 18% (RASS) and 45% (AMS03). The layered method using the RASS and aircraft-based measurements predicts a plume rise that is, on average, nearly half (47 – 49%) of the observed value. In all cases, more than half of the plume rise values are underestimated by more than a factor of 2, and between 22 to 42% of predicted plume rise values are within a factor of 2 of the observations.

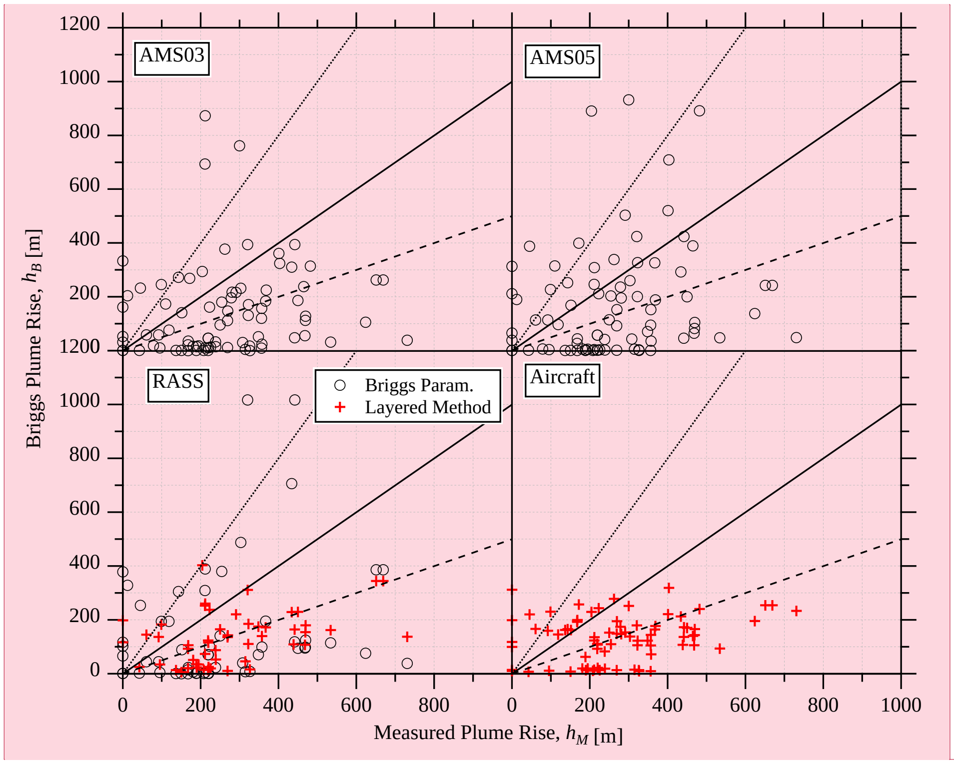

575

Figure 5. Comparison of the predicted plume rise from the Briggs parameterization used in GEM-MACH with the measured plume rise as determined by various atmospheric measurements described in the text. Black circles indicate the Briggs parameterization (Eqns. 1-6) and red crosses indicate the layered method (Eq. 7). Lines demonstrate 2:1 (dotted), 1:1 (solid), and 1:2 (dashed) ratios for comparison.

580

Commented [MG15]: The previous manuscript erroneously plotted “Plume Height” in this figure (not “Plume Rise”). The stack height has been subtracted, resulting in a higher fraction of plume rise values (measured and observed) near zero.

Table 3. Statistics comparing the predicted to measured plume rises using both the Briggs parameterization (Eqns. 1-6) and the layered method (Eq. 7). The intercept (a) and slope (b) of least-squares fit, average calculated ($\overline{h_B}$) and observed ($\overline{h_M}$) plume rises, ratio of all values $\overline{h_B}/\overline{h_M}$, correlation coefficient (r^2), fraction of individual ratios of $h_{B,i}:h_{M,i}$ below the 1:2 ratio (<0.5), within a factor of 2 (>0.5 & <2), and above the 2:1 ratio (>2), and the number (n) of plume to stack matches used for each comparison.

	a [m]	b	r^2	$\overline{h_B}$ [m]	$\overline{h_M}$ [m]	$\overline{h_B}/\overline{h_M}$	Ratio < 0.5	>0.5 & <2	Ratio > 2	n
Briggs Parameterization, Buoyancy Rise Only										
AMS03	104	0.16	0.02	145	263	0.55	54%	32%	15%	82
AMS05	107	0.25	0.04	173	263	0.66	52%	32%	16%	82
RASS	78	0.51	0.07	207	254	0.82	55%	22%	22%	58
Layered Method										
RASS	63	0.24	0.16	130	275	0.47	53%	42%	6%	53
Aircraft	100	0.13	0.06	134	272	0.49	57%	32%	11%	79

Commented [MG16]: Table 3 gives initial results only. The previous manuscript listed results of modified approaches. These are now moved to Table 6 for a much more detailed analysis.

4. Discussion

4.1 Stability Classification

Table 4 lists the frequency of each stability class during box and screen flight times according to each measurement platform as determined by the sign and magnitude of the Obukhov length (L). Stable classification is separated as either due to small positive values of $0 < L < 2h_h$, or stack height above the boundary layer height ($h_s > H$). The RASS and the two towers give similar, predominantly (70 to 94%) neutral, stability during the flights, with RASS indicating the highest frequency (94%) of neutral conditions. Of these three measurement platforms, only the measurements of AMS05 predict plume rise through unstable conditions. We also note that AMS03 and AMS05 are in close spatial proximity to each other (less than 10km), suggesting substantial local changes in stability, again arguing for heterogeneity in the local conditions.

Based on previous studies summarized in VDI (1985), the authors suggested a reduction of the Briggs parameterization by 30% in neutral conditions. Although the atmospheric stability is predominantly classified as neutral in our analysis, we are seeing an underestimation by the Briggs parameterization, in contrast to the previous studies.

Stability was determined using the RASS and aircraft temperature profile measurements based on a comparison of the temperature profile to the adiabatic lapse rate ($\Gamma = g/c_p = 0.0098$ K/m). The temperature profiles were derived from measurements between the minimum aircraft height of 150 m and 300 m (agl). The profile was considered neutral if $-dT/dz$ was within 20% of Γ. Because the RASS profiles demonstrated very different lapse rates near the surface compared to further aloft, these data were separated into near-surface (<100m) and higher (>100m). The profile measurements used for the layered method give a much different indication of stability class, with predominantly stable conditions between for 53% and 89% of the time. The RASS measurement profiles demonstrate a higher frequency of stable conditions near the surface (based on comparison to the lapse rate). For the RASS measurements, there is a significant difference between stability classifications based on Obukhov length compared to stability classifications based on the temperature lapse rate, suggesting that either these two methods are not directly comparable, or that significant spatial heterogeneity exists within the region (as is also implied by the comparison in stability classes noted at AMS03 and AMS05). The layered approach of Eq. 7 is based on the assumption of neutral or stable conditions. For unstable conditions we follow the assumptions outlined in Akingunola et al. (2018) and assume $s = 0$. Since there is a relatively low frequency of unstable conditions in all cases (4% to 13%), any error caused by the assumption of $s = 0$ during unstable conditions is likely small.

Table 4. Frequency of each stability type during flight times determined by each measurement platform. Stability is either determined by parameterization of Obukhov length (L, see Section 2.1), by comparison of the temperature profile with the dry adiabatic lapse rate (Γ), or using the Pasquill-Gifford stability classification scheme (P.-G.).

	Basis	Unstable	Neutral	Stable ($h_s < H$)	Stable ($h_s > H$)
AMS03	L	0%	70%	12%	18%
AMS05	L	26%	66%	2%	6%
RASS	L	0%	94%	0%	6%
RASS (<100m)	Γ	4%	7%	89%	
RASS (>100m)	Γ	13%	33%	53%	
Aircraft (>150m)	Γ	8%	23%	69%	
AMS03	P.-G.	45%	55%	0%	
AMS05	P.-G.	60%	40%	0%	

Commented [MG17]: A comparison to stability determined by the Pasquill-Gifford method is added.

A comparison is also made using the Pasquill-Gifford (Turner and Schulze, 2007) stability class, based on cloud cover and the wind speed at 10-m ($U_{10\text{m}}$). The P-G stability class specifies that during moderate daytime radiation ("a summer day with few broken clouds with the sun 25-60$^{\text{o}}$ above the horizon"), the atmosphere will be unstable (Classes A, B, or C) for wind speeds $U_{10\text{m}}$ < 5 m s^{-1}. For days with some cloud and $U_{10\text{m}} > 5$ m s^{-1} or for completely overcast days, the atmosphere will be neutral (Class D). According to the Pasquill-Gifford system, stable conditions (Classes E, F) will only occur at night (all flights were during daylight hours). Here $U_{10\text{m}}$ is determined from the lowest tower measurements (20 m) and Eq. 11, and cloud conditions are estimated from photographs taken during the flights. This results in predominantly unstable and neutral conditions, as shown in the first two rows of Table 4.

Hence all three methods produce a different prominent stability class: the Obukhov length calculation predicts mostly neutral conditions; the lapse rate predicts mostly stable conditions; and the Pasquill-Gifford stability classes predict an approximately equal occurrence of unstable and neutral conditions. Both the Obukhov length and Pasquill-Gifford class approaches show a substantial difference in the frequency of occurrence of unstable conditions between towers

AMS03 and AMS05, underscoring the local variability which may exist in temperature profiles. In light of this disagreement, we test the change in results with different stability classification schemes in Section 4.4 in order to estimate the extent to which the average plume rise depends on the stability classification.

4.2 Sensitivity to Input Variables

Commented [MG18]: This entire section is redone. Here the testing calculates the difference in plume rise as determined using data from the two towers. This is a test of the sensitivity of the Briggs method to variation specific to this region.

The above analysis suggests the potential for substantial variability between measurement locations, which may be due to heterogeneity of the terrain and surface conditions in the area. Here we perform a simple test of the sensitivity of the Briggs algorithm to uncertainties in input variables due to this variability between measurement platforms. Input variables are modified based on differences between the AMS03 and AMS05 measurement platforms. First, the average plume rise is calculated for the box and screen flight times for the 8 stacks used in the analysis using AMS03 measurements as input. The input variables were then modified by the ratio of the average absolute difference between stations to the mean value (i.e. $\overline{|X_{03} - X_{05}|}/\overline{X}$, where X_{03} and X_{05} are the measurements variables at AMS03 and AMS05 towers respectively, and $\overline{X}$ is the mean value from both stations combined). Instead of modifying the surface temperature ($T_{surface}$) directly, the difference between the air temperature at stack height and surface temperature ($\Delta T = T_a - T_{surface}$) is modified by a fraction, as it is the difference that drives the parameterization (through Eqns. 2, 8, and 10). The average plume rise was then recalculated with the modified variables to determine the resulting change in average plume rise relative to the average plume rise calculated with unmodified input variables.

Table 5. Percent change in average plume height ($\Delta h((1 \pm R)X)/\Delta h(X)$), where X is the modified parameter (i.e. $T_a, U,$ etc.). $\overline{X}$ is the average of each variable from the two tower measurements (AMS03 and AMS05) and $\overline{\Delta X}$ is the average difference. The "Low" value is the average change in plume rise calculated with $(1 - R)X$ and the "High" value is the average change in plume rise calculated with $(1 + R)X$. All averages are for the 46 flight hours (box and screen flight times) and 8 stacks used in the analysis.

Variable	Units	$\overline{X}$	$\overline{\Delta X}$	$R = \overline{\Delta X}/\overline{X}$	Low	High
T_a	K	293.6	0.26	0.1%	1.1%	-2.2%
U	m/s	5.1	0.70	14%	23.1%	-15.6%
$\Delta T = T_a - T_{surface}$	K	-1.4	0.45	31%	-3.9%	3.4%
H	m	1150	990	71%	-27.0%	6.7%
u_*	m/s	0.45	0.06	29%	6.1%	-7.7%
L	m	-132	90	165%	-14.9%	0.3%

Average percentage changes in the plume rise for each modification for each measurement platform are listed in Table 5. The largest differences between the two measurement locations are boundary-layer height (H, 71%) and Obukhov length (L, 165%). This is expected as the parameterizations of Eqns. 9 and 10 are known to be unreliable without heat-flux or upper air measurements. A decrease in boundary-layer height values by 71% leads to an average decrease in the plume rise of 27%, while an increase in boundary-layer height by 71% leads to an average increase in plume rise of 6.7%. Although the average difference in wind speeds between measurement stations is relatively low (14%), this has a considerable impact on the plume rise, ranging from a 23.1% increase to a 15.6% decrease in average plume rise. This is in contrast to air temperature (T_a), temperature difference (ΔT), and friction velocity (u_*), which all results in an average change in plume rise of less than 8%.

The table identifies the variables with the largest impact on the parameterization results, hence which variables require the greatest accuracy when obtained from a meteorological model forecast. These results also help explain the low correlation coefficients of the observation-driven plume rise height comparisons (Table 3), as uncertainty in the estimation of these derived quantities will lead to uncertainty in individual plume rise estimations.

4.3 Horizontal Distance to Plume Rise

If the stacks are physically close enough to the interception of the plume with the box walls or screens it may be the case that the plumes have not travelled a sufficient distance to reach the maximum plume rise that is parameterized by the Briggs algorithms. Briggs (1984) also developed parameterizations of downwind distance to maximum plume rise. A plume in stable conditions will reach its final rise (Briggs, 1984) at

$$x_e = 4.7\left(\frac{U}{\sqrt{s}}\right). \tag{13}$$

A plume in neutral conditions will reach its final rise (Briggs, 1975) at

$$x_e = \begin{cases} 49F_b^{5/8} & \text{for } F_b < 55\ \mathrm{m^4s^{-3}} \\ 119F_b^{2/5} & \text{for } F_b > 55\ \mathrm{m^4s^{-3}} \end{cases} \tag{14}$$

In unstable conditions, the plume fumigates and is evenly distributed in concentration between the surface and a height of $1.5\Delta h$, based on the assumption that the half-width of the plume is $0.5\Delta h$. Although no parameterization has been developed for the distance required to reach maximum plume rise in unstable conditions, Briggs (1984) provides a parameterization of the average horizontal distance to fumigation (contact of the plume with the surface) as

$$x_f = \frac{U}{w}(h_s + 0.5\Delta h), \tag{15}$$

where the average downdraft speed is $w = 0.8u_*$, following Briggs (1984).

Using the AMS03 input data as an example, none of the 87 matched plumes have distance from stack to measurement location (x_d) less than the horizontal distance to reach maximum plume rise ($x_d < x_e$) in neutral or stable cases, and there are no unstable cases (Table 4). As discussed above, the analysis is limited to plume sources that are within 50 km of the box walls or screens.

The distances between stacks and box walls (following the forward trajectories) range from 4 to 16 km, while the distances between stacks and screens ranges from 3 km to more than 150 km. There are 8 screens located with within 40 km of the stack sources and 12 screens located more than 60 km of the stack sources (there are none in the 40 – 60 km range). Tests demonstrate (discussed in the next section) that including the 12 screen plume observations beyond 60 km from the sources in the analysis results in lower correlations and poorer performance of the Briggs parameterizations, as expected.

Given that the observed plume rise is generally much higher than the calculated plume rise, it should also be the case that distance to maximum plume rise is also underestimated. If it is assumed that the plume reaches its maximum height at the measurement location and the predicted plume rise (h_B) is less than the measured plume rise (h_M), then the actual distance to maximum plume rise can be calculated as $x_e' = x_e\, h_M/h_B$. Using this modified distance to plume rise, 13% of the plumes have distance to maximum plume rise greater than the distance between stack and screen (or box wall). This indicates that for these plumes, the assumption that $x_e' = x_d$ is incorrect and the maximum rise for these plumes is higher than h_M. Hence, the parameterized plume rise may underestimate the actual plume rise in some cases due to the measured plumes not reaching their maximum height. This magnitude of the underestimation is investigated as one of the modifications discussed below.

Commented [MG19]: Since the observed plume heights are much higher than the calculated plume heights, the potential effect of underestimation of distance to plume rise is investigated.

4.4 Modifications to the Plume Equations

Commented [MG20]: The following section is a new analysis that tests multiple modifications to the plume rise algorithm. In the previously submitted manuscript only the “Minimum Criteria” (now a subset of Section 4.4.3) and “Effluent Momentum” (Section 4.4.4) were compared.

To investigate the underestimation of plume rise by the parameterization, we recalculate the predicted plume rise with a number of modifications. For ease of comparison, we use only the AMS03 tower data to drive the algorithm. Table 6 lists the results of these modifications. The “base case” is the analysis as described in the preceding sections with no modifications. The “base case” statistics are reprinted in Table 6 (case 0) from the first line of Table 3 in order to facilitate comparison. The results are presented as scatter plots for each case (following Fig 5.) in the supplementary material. Each of the comparison studies presented as different cases in Table 6 are described in more detail in the sub-sections which follow.

4.4.1 Separation of Individual Stacks

Cases 1 through 8 in Table 6 provide statistics for the stack-plume matching separated by each of the 8 stacks as listed in Table 2. Half of the stacks demonstrate very strong underestimation of plume rise, with ratios of calculated to observed plume rise between 4% and 13%. In the cases of the Suncor stacks (1 and 3), these are large diameter stacks ($d_s = 5.8$ and 7.0 m, see Table 1) with very low effluent exit velocities. The average exit velocity of these stacks over the duration of the flights was $w_s < 0.1$ m s^{-1} (Table 1). The CNRL stacks, by comparison, have relatively moderate and small diameters (3.4 m and 1.4 m) and moderate exit velocities (averages of 4.1 and 6.2 m s^{-1} over the flight durations). This suggests that the underestimation of the plume height may result from either (inaccurately) low estimates of volume fluxes from these facilities, or that plume rise equations themselves are unsuitable for stacks with these conditions. This does not appear to be the case for the CNRL stacks. However, there are only two stack-plume matches for each CNRL stack, so this is not a very statistically representative sample.

Table 6. Statistics comparing the predicted to measured plume rises using the Briggs parameterization (Eqns. 1-6) with either select conditions only or modification to the analysis. Cases are described in further detail in the text. Variables are defined as in Table 3.

Case	#	a [m]	b	r^2	$\overline{h_B}$ [m]	$\overline{h_M}$ [m]	$\overline{h_B}/\overline{h_M}$	Ratio < 0.5	>0.5 & <2	Ratio > 2	n
Base Case	0	105	0.14	0.02	143	265	0.54	55%	30%	14%	83
Suncor 1	1	1	0.03	0.32	6	178	0.04	91%	0%	9%	11
Suncor 2	2	140	-0.01	0.00	137	260	0.52	73%	9%	18%	11
Suncor 3	3	8	0.00	0.00	9	199	0.04	92%	0%	8%	12
Suncor 4	4	235	-0.21	0.02	175	286	0.61	50%	33%	17%	12
Syncrude 1	5	289	0.02	0.00	294	296	1.00	18%	53%	29%	17
Syncrude 2	6	149	0.12	0.04	185	298	0.62	25%	69%	6%	16
CNRL 1	7	66	-0.04	N/A	49	395	0.13	100%	0%	0%	2
CNRL 2 (NPRI)	8	100	-0.23	N/A	15	374	0.04	100%	0%	0%	2
Neutral Cases Only	9	101	0.13	0.01	134	244	0.55	56%	26%	18%	50
Stable Cases Only	10	116	0.14	0.04	157	296	0.53	55%	36%	9%	33
Expanded Neutral Limits	11	105	0.14	0.02	143	265	0.54	55%	30%	14%	83
Reduced Neutral Limits	12	94	0.16	0.03	136	265	0.51	55%	30%	14%	83
Stability by Lapse Rate	13	93	0.14	0.05	129	265	0.49	55%	33%	12%	83
Stability by P-G. Class.	14	140	0.24	0.02	203	265	0.77	48%	33%	19%	83
Incl. $x_e > 50$km	15	126	-0.01	0.00	123	306	0.40	63%	24%	13%	121
Scaled to Max. Dist.	16	107	0.14	0.02	145	265	0.55	55%	30%	14%	83
No limit of -5K/km	17	109	0.16	0.02	151	265	0.57	53%	31%	16%	83
Eqns 4b and 5b (no min)	18	1416	-1.25	0.00	1085	265	4.10	54%	23%	23%	83
Alternate Neutral Eq. 16	19	4422	-4.26	0.00	3293	265	12.44	51%	23%	27%	83
Momentum (Eq 17 & 18)	20	114	0.17	0.02	159	265	0.60	54%	30%	16%	83
Momentum (Eq 20)	21	227	0.40	0.02	333	265	1.26	48%	17%	35%	83

Only the calculated to observed plume matches that originate from Syncrude1 (case 5) demonstrate good agreement between the Briggs equations and the observations (with an average ratio of 1.0 and more than half the calculated plume rise values with a factor of 2 of the observed plume rise values. This stack is the largest of the 8 stacks ($h_s = 183$ m, $d_s = 7.9$ m) and also has the highest average effluent exit velocity ($w_s = 12.0$ m s^{-1}). This suggests that the Briggs parameterization (as used in the GEM-MACH model) demonstrates better prediction with relatively larger stacks (>180 m) with higher volume flow rates (>500 m^3 s^{-1}). Based on 2010 inventory values, this stack emits 10 times more SO$_2$ than any of the other reported stacks. The resulting higher downwind concentrations would likely make observed plume much easier to location and identify accurately. For this Syncrude1 stack, the correlation coefficient and slope of the best fit for the 17 stack-plume matches are not significantly different from zero. Hence, while the overall average plume rise for this stack appears accurate, the equations do not predict individual cases of plume rise well.

4.4.2 Stability

Three types of tests were done to determine the effect of atmospheric stability classification on the calculated plume rise: separation by stability class (cases 9 and 10), testing of sensitivity to the limits of neutral classification (cases 11 and 12), and testing of other stability classification methods (cases 13 and 14). These tests are described in more detail below.

We first compare the calculated to observed plume rise values which occur during neutral conditions only (case 9) and stable conditions only (case 10), with stability is based on Obukhov length. For the times when plumes were observed (and matched to stack sources), there were no unstable classifications using the AMS03 tower site data (based on Obukhov length). There are 50 stack-plume matches during neutral conditions and 33 stack-plume matches during stable conditions. There is no significant difference between the stack-plume comparisons for the plume rise under neutral conditions versus stable conditions. The ratio of average predicted plume rise to observed plume rise is similar in both cases (0.55 compared to 0.53), and the fraction of plume rise values less than one-half the observed values is near 55% in both cases. Hence, the underestimation of plume rise does not seem to be dependent on predicted stability classification.

Secondly, the sensitivity of the results to the limits of neutral conditions ($-4 < h_s/L < 0.5$) is tested by doubling the limit values (case 11: $-8 < h_s/L < 1.0$) and halving the values (case 12: $-2 < h_s/L < 0.25$). The results demonstrate that the calculated plume rise values are not strongly dependent on the choice of limits. Doubling the limits does not change the statistics relative to the base case, as it results in no changes in stability classification. Halving the limits results in a slightly lower average calculated plume rise value (136 m compared to the 143 m base case) due to the reclassification of 5 stack-plume matches from neutral to unstable.

Finally, the results discussed in Section 4.1 suggest that there is poor agreement between the various methods used to classify stability. As discussed previously, the estimation of Obukhov length based on the bulk Richardson number may be considered less accurate than an estimation based on heat flux measurements. We recalculate the plume rise values using the stability classification based on the comparison of the negative temperature gradient, $-dT/dz$, to lapse rate, Γ, (case 13) and again using the Pasquill-Gifford stability classification based on cloud observations and wind speed (case 14). The use of the lapse rate classification results in a designation of predominantly stable conditions (Table 4). This results in a small change in average calculated plume height and a similar distribution of plume rise values compared to the base case (with stability conditions based on the stability parameter, h_s/L). Use of the Pasquill-Gifford stability classification results in a mix of either neutral or unstable conditions. This reclassification of atmospheric stability results in a better agreement between calculated and observed plume rise values, with an average ratio of 0.77. However, nearly half (48%) of the calculated plume rise values are below 50% of the observed values, suggesting there is still significant underestimation of plume rise, even with this reclassification of atmospheric stability.

4.4.3 Plume Rise Calculation Modifications

A number of modifications were made to test the sensitivity of the results to various assumptions and equations used to calculate plume rise in the base case. These include the assumption of validity of the equations beyond a given downwind distance (case 15), the estimation of maximum plume height for plumes may still be ascending at the measurement location (case 16), the effect of limits and minima used in the equations (cases 17,18), and finally an alternate plume rise equation used for neutral conditions (case 19).

Firstly, as discussed above, the distance between the stack and the horizontal point of measurement of plume height is limited in this analysis to less than 50 km. Removal of this criteria (case 15) adds a further 38 stack-plume matches to the original 83 stack-plume matches in the base case. The observed plume rise values of these distant plumes are generally higher, and the predicted plume rise values are lower. The resulting average ratio of calculated to observed is 0.40 (compared to 0.54 for the base case which only includes plumes that have travelled less than 50 km before measurement).

As discussed in Section 4.3, the calculated distance to maximum plume rise is less than the distance between the stack and the measurement location for all stack-plume matches. However, when the distance to maximum plume rise is modified by a factor equal to the ratio of observed plume rise to calculated plume rise, approximately 13% of the plumes should reach maximum plume height further from the stack than the measurement location. To test whether this is causing an underprediction of plume rise, we adjust the calculated plume rise values for those plumes with $x_e' > x_d$ by the ratio of adjusted distance to maximum plume rise to stack-to-measurement distance ($h_B' = h_B\, x_e'/x_d$). This is shown in Table 6 as case 16. The difference in statistics between this case and the base case is negligible, suggesting that the underprediction of plume rise is not due to the observation of plumes which are still ascending.

The −5 K/km minimum value of dT/dz used to calculate s (Eq. 2) could potentially limit the plume rise. Steeper negative temperature gradients result in a smaller value of s, which would result in higher plume rise under stable conditions. This condition is removed (case 17) and the resulting statistics are compared in Table 6. This results in a slightly higher predicted plume rise, with an average ratio of 0.57 (compared to 0.54 for the base case). Hence these results do not appear to be sensitive to this minimum value.

As discussed in Section 2.1, the minimum criteria of Eqns. 4 and 5, which are used in the GEM-MACH model are not used in other plume rise models, such as SMOKE. To investigate the difference between these two approaches, the plume rise is recalculated (case 18) using only the second (rightmost) term within the minimum functions of Eqns. 4 and 5. The resulting statistics are listed in Table 3. The removal of the minimum function results in 3 cases of extremely (i.e. unrealistically) high plume rise (between 6 and 41 km), all of which occur in neutral conditions. Because of these extreme values, the ratio of average predicted to average observed plume rise is

4.1. However, the majority of predicted values (54%) are less than half of the observed plume rise values (similar to the base case), suggesting that the high ratio of predicted to observed value is due to a few outliers. This implies that a lower limit on wind speed and friction velocity should be used to prevent unrealistically high plume rise values when using these equations without the minimum functions, making the GEM-MACH choice of minima appropriate.

In order to test other parameterizations of plume rise, the equation for plume rise in neutral conditions (Eq. 3) is replaced by an alternative equation (De Visscher, 2013), given as

$$\Delta h = \frac{400F_B}{U^3}. \tag{16}$$

The alternative equation is tested as case 19. For cases with moderately low wind speeds ($2 < U < 3$ m s^{-1}), the equation gives plume rise as high as 6 km, while for very low wind speeds ($U < 1$ m s^{-1}), plume rise higher than 100 km is predicted. This suggests this equation should be limited to cases of neutral conditions with high wind speeds, and it may be better suited for stability classification using the Pasqill-Gifford scale, which requires higher wind speeds for neutral stability classification (for non-overcast conditions).

4.4.4 Effluent Momentum

The plume rise due to momentum of stack effluent is not included in the parameterization used in GEM-MACH (see Section 2.1). To investigate whether neglect of momentum rise may be a significant contribution to the underestimation of plume rise we test two sets of equations to include this effect. Plumes are typically classified as either momentum driven or buoyancy driven, and the maximum of Δh and Δh_m is used to estimate plume rise (e.g. Briggs, 1984; VDI, 1985). As a first test, we add Δh and Δh_m together to give an upper limit of plume rise due to both momentum and buoyancy. As a second test, we use a parameterization (De Visscher, 2013) that includes both effects simultaneously.

For the first test (case 20), parameterizations for momentum-dominated plumes developed by Briggs are given in De Visscher (2013) for stable and neutral conditions respectively as

$$\Delta h_m = 1.5\left(\frac{F_m}{Us^{1/2}}\right)^{1/3}, \quad \Delta h_m = 3\left(\frac{F_m}{U^2}\right)^{1/2}, \tag{17,18}$$

where the momentum flux is

$$F_m = \left(\frac{T_a}{T_s}\right)\frac{d_s^2 w_s^2}{4}. \tag{19}$$

A parameterization of the plume rise due to momentum during unstable conditions is not required here as there are no cases of plume matching during unstable conditions using the AMS03 tower data used for this comparison. Eqns. 17 and 18 are meant for plume rise due to momentum only (without buoyancy). Here we add the plume rise due to momentum to the plume rise due to buoyancy as $h_B = \Delta h + \Delta h_m$. This results in a slight improvement in predicted plume rise (ratio of 0.60 compared to the base case of 0.54), but the majority (54%) of predicted plume rise values are less than half the observed values.

For the second test (case 21) we follow the approach used in the CALPUFF model in which buoyancy and momentum are considered simultaneously (De Visscher, 2013). For plume rise in neutral or stable conditions, the plume rise can be calculated as

$$\Delta h = \left(\frac{3F_m x_e}{\beta^2 U^2} + \frac{8.3F_b x_e^2}{U^3}\right)^{1/3} \quad (20)$$

where x_e is given by Eq. 15 and $\beta = 1/3 + U/w_s$. The CALPUFF model limits the wind speed at stack height (U) used in Eq. 20 to a minimum of 1 m s^{-1}. Including this limit in our analysis had negligible effect on the resulting plume rise values. Statistics for this analysis are shown in Table 6 as case 21. The ratio of average predicted to observed values (1.26) suggests an overestimation of plume rise with this method. Nearly half (48%) of the predicted plume rise values are less than half the observed values and a large fraction (34%) of the predicted plume rise values are more than double the observed values. Hence this method seems to both overestimate and underestimate a large fraction of plume rise values, but the average predicted plume rise is closer to the average observed predicted plume rise compared to the GEM-MACH parameterization of buoyancy only.

5. Conclusions

These results demonstrate a significant underestimation of plume rise using the Briggs plume rise parameterizations. The ratio of average modelled plume rise to average measured plume rise ($\overline{h_B}/\overline{h_M}$) varies from 0.55 to 0.82 using Briggs parameterization with the tower or RASS used to measure input variables. The ratio $\overline{h_B}/\overline{h_M} = 0.47$ or 0.49 using the layered method with either the RASS of the aircraft used to measure input variables. This range of ratios suggests an average underestimation between 18 and 53%. Results are improved slightly when atmospheric stability is classified using the Pasquill-Gifford system, which improves the ratio from 0.55 using the AMS03 tower with stability classified according to stability parameter (h_s/L) to 0.77 using the Pasquill-Gifford system. Results are also improved by including plume rise due to momentum at the stack exhaust (Eq. 20), although this results in some overprediction of plume rise, with an average ratio of $\overline{h_B}/\overline{h_M} = 1.26$ using the AMS03 tower data.

Commented [MG21]: This was 0.51 to 0.87 in the previous manuscript.

These results are in direct contrast to the many studies summarized in VDI (1985), which consistently suggest that plume rise is overestimated by the Briggs equations. The more recent study of Webster and Thomas (2002) might possibly imply an underestimation of plume rise, owing to an overestimation of surface concentration measurements using a plume rise model; however there may be other reasons for this overestimation unrelated to plume rise. The authors of the VDI report suggest that the Briggs parameterization should be reduced by a factor of 30% in neutral conditions in order to better match observations. In contrast to this suggestion, our results would be improved significantly by increasing the Briggs parameterization by a factor of 30%.

Much of the underestimation in this study appears to be driven by two stacks (Suncor 1, 3) which have relatively low effluent exit velocities. Based on a 2010 CEMA inventory, these stacks are among the list of significant SO_2 emitters (0.14 and 0.19 kg s^{-1}), although since these are yearly average inventory values, there is a possibility that the stacks were not emitting significant SO_2

during this specific study period. Although there is also the possibility that the plumes from these stacks are below the lowest aircraft measurement height of 150 m (and hence not observed), given the stack heights of 107 and 137 m this seems unlikely.

Commented [MG22]: The disaggregation of individual stacks is added to this revised manuscript.

By far, the best results of the Briggs parametrization (as used in the GEM-MACH model) are for the largest, Syncrude1 stack. This stack emits between 11 and 40 times more SO_2 (2.2 kg s^{-1}) than the other stacks. Although the Briggs parameterization performs poorly for the smaller and moderately sized stacks, it performs well for the large stack responsible for approximately ¾ of the total emissions. Hence, any air quality assessments using the Briggs parametrization in this region should be reasonably accurate and future improvements to the algorithms should focus on the relatively smaller stacks.

For both the Briggs parameterization and layered method and for all the measurement platforms used in this study, the correlation of parameterized plume rise to measured plume rise is low ($r^2 \leq 0.2$) and the slopes of the least-squares fits are generally less than 0.5. Carson and Moses (1969) stated that “no plume rise equation can be expected to accurately predict short term plume rise” and that their parameterizations were “to be used for general design considerations.” This statement appears to remain true nearly 50 years later and the wide use of these same equations in air quality models indicates that little improvement has been made.

The aircraft-based measurements used for this study provide only a “snapshot” of plume rise and atmospheric conditions as measurements are made on a timescale of a few hours in the morning or afternoon over the course of a few weeks in summer. However, this consistent underestimation of plume height for these observations suggest that further investigation is warranted. Given the advancements in atmospheric measurement technology in recent decades (e.g. automated lidar, RASS, image analysis), there is an opportunity to make long-term measurements of plume rise and atmospheric conditions in an effort to improve predictability. Although the Briggs algorithms have been in use for nearly 4 decades, are used in many air-quality models (e.g. GEM-MACH, AEROPOL, SCREEN3, CALGRID, RADM, SMOKE, and SMOKE-EU), and are widely referenced in air quality and dispersion texts (Beychok, 2005; Arya, 1998), the verification of these algorithms relies on decades old measurement techniques. More in-situ measurements of plume height are clearly needed to attempt to quantify the uncertainties in these parameterizations and to suggest improvements to the algorithm.

Further, these observations suggest the presence of considerable horizontal heterogeneity in meteorological conditions across this region, with towers within a 10km distance providing substantially different statistics of stability conditions during the study period. This suggests that meteorological observations in close proximity to the stacks may be needed to further improve the algorithms. We examine the potential impact of this heterogeneity in our companion paper (Akingunola et al, 2018) using a high resolution meteorological model.

Commented [MG23]: Here a mention of the potential contribution of heterogeneous conditions is added, which ties in to the investigation of our companion paper.

Acknowledgements

The authors wish to thank the Wood Buffalo Environmental Association (WBEA) for the use of the Lower Camp Met Tower (AMS03) and Mannix Tower (AMS05) data. The Continuing

Emission Monitoring System (CEMS) data were provided by Marilyn Albert, Ewa Przybylo-Komar, Katelyn Mackay, and Tara-Lynn Carmody of Data Management and Stewardship, Corporate Services Division, Alberta Environment and Parks. Funding for the aircraft measurement study was provided by Environment and Climate Change Canada and the Oil Sands Monitoring Program

References

A. Akingunola, P.A. Makar, M.D. Moran, J, Zhang, Q. Zheng, S.-M. Li (2017), Simulations of Oil Sands Emissions, Transformation and Fate using the GEM-MACH Model: The impacts of plume rise and particle size resolution. *Atmos. Chem. Phys.* This issue.

S.P. Arya (1998) Air Pollution Meteorology and Dispersion (1st ed.). Oxford University Press.

M.R. Beychok (2005). Fundamentals Of Stack Gas Dispersion (4th ed.). author-published

J. Bieser, A. Aulinger, V. Matthias, M. Quante, P. Builtjes (2011a) SMOKE for Europe – adaptation, modification and evaluation of a comprehensive emission model for Europe. *Geoscientific Model Development*, 4, 47-68. doi:10.5194/gmd-4-47-2011

J. Bieser, A. Aulinger, V. Matthias, M. Quante, H.A.C. Denier van der Gon (2011b) Vertical emission profiles for Europe based on plume rise calculations, *Environ. Pollut.*, 159, 2935-2946. doi:10.1016/j.envpol.2011.04.030

G.A. Briggs (1969) Plume rise. Report for U.S. Atomic Energy Commission, Division of Technical Information.

G.A. Briggs (1975) Plume rise predictions, Lectures on air Pollution and environmental impact analyses. In: Workshop Proceedings, Sept. 29-Oct. 3, pp. 59-111. Boston, MA, USA.

G.A. Briggs (1984) Plume rise and buoyancy effects, atmospheric sciences and power production. In: Randerson, D. (Ed.), DOE/TIC-27601 (DE84005177), TN. Technical Information Center, U.S. Dept. of Energy, Oak Ridge, USA, p. 850.

G,A, Briggs (1985) Analytical parameterizations of diffusion: the convective boundary layer, *J. Clim. Appl. Meteorol.*, 24, 1167–1186.

B. Bringfelt (1968) Plume rise measurements at industrial chimneys. *Atmos. Environ.* 2, 575-598.

D.W. Byun, F.S. Binowski (1991) Sensitivity of RADM to point source emissions processing. In: Paper 5.4 presented at the 7th Joint conference on Applications of Air Pollution Meteorology with the Air and Waste Management Association, Jan. 14-18, 1991, New Orleans, LA. American Meteorological Soc, Boston, MA, USA, pp. 70e73.

D.W. Byun, J.K.S. Ching (1999) Science algorithms of the EPA Models-3 community multiscale air quality (CMAQ) modeling system, US EPA, Office of Research and development, EPA/600/R-99/030.

J.E. Carson and H. Moores (1969) The Validity of Several Plume Rise Formulas, *J. Air Pollut. Contr. Assoc.*,19:11, 862-866, doi:10.1080/00022470.1969.10469350

CEMA (2012) Lower Athabasca Region Source and Emission Inventory, Prepared for Cumulative Environmental Management Association, Ft McMurray, AB, April 16, 2012, ENVIRON CA12-00394A, Stantec 123510559 (T210).

CEMS (1998) Continuous Emission Monitoring System (CEMS) Code, Alberta Environmental Protection, Pub. No. Ref. 107, ISBN: 0-7732-5038-7.

CMAS Website, https://www.cmascenter.org/smoke/, last accessed Feb., 2018.

J. Côté, S. Gravel, A. Méthot, A. Patoine, M. Roch, and A. Staniforth (1998) The Operational CMC–MRB Global Environmental Multiscale (GEM) Model. Part I: Design Considerations and Formulation. *Mon. Weather Rev.*, 126, 1373–1395, doi: 10.1175/1520-0493(1998)126<1373:TOCMGE>2.0.CO;2.

J. Cuxart, J. Cunillera, M.A Jiménez, D. Martínez, F. Molinos, J.L. Palau (2011) Study of Mesobeta Basin Flows by Remote Sensing, *Bound.-Lay. Meteor*. 143 (1), 143-158. doi:10.1007/s10546-011-9655-8

A. De Visscher (2013) Air Dispersion Modeling: Foundations and Applications. Wiley. pp 664.

ECCC & AEP (2016) Environment and Climate Change Canada & Alberta Environment and Parks: Joint Oil Sands Monitoring Program Emissions Inventory Compilation Report, http://aep.alberta.ca/air/reports-data/documents/JOSM-EmissionsInventoryReport-Jun2016.pdf, 146 pp, last accessed Nov., 2017.

C. Emery, K. Jung, G. Yarwood (2010) Implementation of an Alternative Plume Rise Methodology in CAMx. Final Report, Work Order No. 582-7-84005-FY10-20.

W.G. England, L.H. Teuscher, R.B. Snyder (1976) A measurement program to determine plume configurations at the Bear Gas Turbune Facility, Port Westward, Oregon. *J. Air. Poll. Contr. Assoc.* 10, 986-989.

J.R. Garratt (1994) The atmospheric boundary layer (1st ed.). Cambridge University Press.

J. Gielbel (1979) Messungen der Abgasfahnenüberhöhung eines Steinkohlekraftwerkes mit Hilfe von LIDAR (Plume Rise measuremetns of a pit coal power plant by means of LIDAR). (German) Schriftenreihe der Landesanstalt fur Immissionsschutz des Landes NRW, Heft 47, S. 42/59.

M. Gordon, S.-M. Li, R. Staebler, A. Darlington, K. Hayden, J. O'Brien, M. Wolde (2015) Determining air pollutant emission rates based on mass balance using airborne measurement data over the Alberta oil sands operations, *Atmos. Meas. Tech.*, 8, 3745-3765, doi:10.5194/amt-8-3745-2015.

P.M. Hamilton (1967) Paper III: plume height measurements at Northfleet and Tilbury power stations. *Atmos. Environ.*, 1, 379-387.

N.S. Holmes, L. Morawska (2006) A review of dispersion modelling and its application to the dispersion of particles: An overview of different dispersion models available. *Atmos. Environ.* 40 (30), 5902-5928. doi: 10.1016/j.atmosenv.2006.06.003.

M.R. Houyoux (1998) Technical Report: Plume Rise Algorithm Summary for the Sparse Matrix Operator Modeling System (SMOKE). North Carolina Department of Environment and Natural Resources, UNC, Chapel Hill, North Carolina, ENV-98TR004eTR0v1.0.

J.C. Kaimal and J.J. Finnigan (1994) Atmospheric Boundary Layer Flows: Their Structure and Measurement (1st ed.), Oxford University Press.

S.-M. Li, A. Leithead, S.G. Moussa, J. Liggio, M.D. Moran, D. Wang, K. Hayden, A. Darlington, M. Gordon, R. Staebler, P.A. Makar, C. Stroud, R. McLaren, P.S.K. Liu, J. O'Brien, R. Mittermeier, J. Zhang, G. Marson, S. Cober, M. Wolde, J. Wentzell (2017) Differences between Measured and Reported Volatile Organic Compound Emissions from Oil Sands Facilities in Alberta, Canada. *Proc. Natl. Acad. Sci.*, 114, 19, E3756-E3765. doi: 10.1073/pnas.1617862114

J. Liggio, S.-M. Li, K. Hayden, Y.M. Taha, C. Stroud, A. Darlington, B.D. Drollette, M. Gordon, P. Lee, P. Liu, A. Leithead, S.G. Moussa, D. Wang, J. O'Brien, R.L. Mittermeier, J. Brook, G. Lu, R. Staebler, Y. Han, T.T. Tokarek, H.D. Osthoff, P.A. Makar, J. Zhang, D. Plata, D.R. Gentner (2016) Oil sands operations are a major source of secondary organic aerosols, *Nature*, 534, 91–94. doi:10.1038/nature17646.

NPRI website, http://ec.gc.ca/inrp-npri, last accessed Feb., 2018.

P.A. Makar, W. Gong, J. Milbrandt, C. Hogrefe, Y. Zhang, G. Curci, R. Zakbar, U. Im, S. Galmarini, S. Gravel, J. Zhang, A. Hou, B. Pabla, P. Cheung, R. Bianconi (2015a) Feedbacks between air pollution and weather, part 1: effects on weather, *Atmos. Environ.*, 115, 442-469.

P.A. Makar, W. Gong, C. Hogrefe, Y. Zhang, G. Curci, R. Zabkar, J. Milbrandt, U. Im, A. Balzararini, R. Baró, R. Bianconi, P. Cheung, R. Forkel., S. Gravel, M. Hirtl, L. Honzak, A. Hou, P. Jiménez-Guerrero, M. Langer, M.D. Moran, B. Pabla, J.L. Pérez, G. Pirovano, R. San José, P. Tuccella, J. Werhahn, J. Zhang, S. Galmarini (2015b). Feedbacks between air pollution and weather, part 2: Effects on chemistry, *Atmos. Environ.*, 115, 499-526.

L. Mahrt (1981) Modelling the depth of the stable boundary-layer. *Bound.-Lay. Meteor.*, 21, 3–19. doi:10.1007/BF00119363.

D.J. Moore (1974) A comparison of the trajectories of rising buoyant plumes with theoretical/empirical models. *Atmos. Environ.*, 8, 441-457.

B.E Rittmann (1982) Application of two-thirds law to plume rise from industrial-sized sources. *Atmos. Environ.*, 16, 2575-2579.

G. Sharf, M. Peleg, M. Livnat, M. Luria (1993) Plume rise measurements from large point sources in Israel, *Atomos. Environ.*, 27A, 1657 – 1663. doi.org/10.1016/0960-1686(93)90228-Q

D.B. Turner, R.H. Schulze (2007) Practical guide to atmospheric dispersion modeling. Dallas, Texas, USA: Trinity Consultants, Inc. and Air & Waste Management Association.

VDI (1985) Ausbreitung von Luftverunreinigungen in der Atmosphäre; Berechnung der Abgasfahnen-überhöhung. (Dispersion of air pollutants in the atmosphere; determination of plume rise) 1985-06 (German/English), Kommission Reinhaltung der Luft (KRdL) im VDI und DIN – Normenausschuss, Available from: http://www.vdi.de.

H.N. Webster, D.J. Thomson (2002) Validation of a Lagrangian model plume rise scheme using the Kincaid data set. *Atmos. Environ.*, 36, 5031–5042.

J. Zhang, M.D. Moran, Q. Zheng, P.A. Makar, P. Baratzadeh, G. Marson, P. Liu, and S.M. Li. Emissions preparation and analysis for air quality modelling for the JOSM project over the Athabasca oil sands region of Alberta, Canada, *Atmos. Chem. Phys.* This issue.